ACCSCIENCE PUBLISHING

International Journal of Bioprinting

REVIEW ARTICLE

Artificial intelligence in 3D bioprinting: From predictive modeling to autonomous biofabrication

Jooyoung Lee[1] and Hyungseok Lee[1,2]*

[1]Department of Smart Health Science and Technology, Kangwon National University, Chuncheon, Gangwon State, Republic of Korea

[2]Department of Mechanical Convergence Engineering, Kangwon National University, Chuncheon, Gangwon State, Republic of Korea

Abstract

Three-dimensional bioprinting is shifting from empirically tuned fabrication toward workflows that integrate quantitative data on materials, printing, structure, and biology. This review summarizes how artificial intelligence (AI) and machine learning are being used across these areas, with particular attention to studies that include experimental validation. We first discuss conventional measurements such as rheology, filament formation, shape fidelity, and biological assays because these measurements define the inputs and labels used by AI models. We then examine how data from materials, processes, structures, and biology can be linked within the same experiment. Representative studies are compared with respect to the models used, the amount and type of data, validation methods, and whether model outputs were tested in new experiments. Current evidence is strongest for printability prediction, structural quality assessment, and image-based monitoring, while several studies have also demonstrated cell-viability prediction, parameter optimization, transfer learning, Bayesian optimization, and closed-loop correction. We also discuss inverse design, active learning, uncertainty-aware optimization, physics-informed learning, and biological feedback as approaches to reducing the experimental burden. Finally, we use a five-level maturity framework to distinguish AI-assisted analysis, AI-driven recommendations, adaptive control, and autonomous biofabrication. AI is increasingly influencing experimental planning and process control, but fully integrated autonomous workflows remain uncommon. Further progress will depend on validation across materials and platforms, longer-term biological readouts, traceable data, and the reliable integration of experimental feedback.

Keywords: Machine learning; Bioink printability; Multimodal data; Process monitoring; Inverse design; Self-driving laboratory

***Corresponding author:**
Hyungseok Lee
(ahl@kangwon.ac.kr)

Citation: Lee J, Lee H. Artificial intelligence in 3D bioprinting: From predictive modeling to autonomous biofabrication. *Int J Bioprint*. doi: 10.36922/IJB026380407

Received: September 15, 2026

Revised: October 22, 2026

Accepted: October 27, 2026

Published online: November 16, 2026

Copyright: © 2026 Author(s). This is an Open-Access article distributed under the terms of the Creative Commons Attribution License, permitting distribution, and reproduction in any medium, provided the original work is properly cited.

Publisher's Note: AccScience Publishing remains neutral with regard to jurisdictional claims in published maps and institutional affiliations.

1. Introduction

Three-dimensional (3D) bioprinting occupies a distinctive position within biofabrication because it combines controlled manufacturing with the deliberate organization of living matter.[1] Consequently, a printed construct cannot be evaluated solely by how closely it resembles a digital design at the time of fabrication. After printing, the deposited

matrix continues to swell, crosslink, degrade, remodel, and exchange mass with the surrounding medium, while encapsulated or deposited cells migrate, proliferate, differentiate, and secrete new extracellular matrix.[2] The quality of a bioprinted construct is therefore intrinsically time-dependent. A construct that initially exhibits acceptable geometry may lose dimensional stability during culture, whereas one that initially deviates from its nominal geometry may subsequently support useful biological remodeling.[3] Accordingly, the broad definition of biofabrication places bioprinting at the intersection of manufacturing, biomaterials engineering, and cell biology rather than treating it as a direct biological analog of conventional polymer printing.[4]

Printability is similarly multidimensional.[5] Continuous extrusion alone does not constitute successful printing. A material may produce a stable filament yet exhibit excessive fusion at filament intersections, collapse across unsupported gaps, or fail to maintain layer height during repeated deposition.[6] Conversely, a formulation with excellent geometric retention may require excessive extrusion pressure or crosslinking conditions that compromise cellular performance. Printability and shape fidelity are therefore increasingly evaluated using combinations of rheological behavior, filament formation, pore geometry, collapse, fusion, and biological compatibility rather than a single universal scalar value.[7] Such standardized assessment is particularly important for artificial intelligence (AI) because the reliability of machine learning (ML) outputs is inherently constrained by the quality of the experimental labels used for training.[8]

Optimization consequently remains one of the most persistent practical bottlenecks in bioprinting. Conventional workflows often involve sequential variation of polymer concentration, crosslinker or photoinitiator content, nozzle diameter, extrusion pressure or flow rate, translation speed, temperature, layer height, and crosslinking dose. Although such screening is necessary when introducing a new bioink, the resulting operating window can remain strongly dependent on hydrogel lot, cartridge geometry, printer calibration, cell concentration, preparation history, ambient conditions, and image analysis procedures. As the number of interacting variables increases, the experimental design space expands rapidly, making one-factor-at-a-time optimization increasingly inefficient.[9] Moreover, identical nominal machine settings can produce different physical outcomes when material rheology or dispensing-system compliance changes. The parameter table recorded in a protocol therefore captures only part of the process state responsible for generating a construct.

Early discussions of ML in bioprinting recognized these limitations and proposed data-driven analysis as a means of moving beyond repeated empirical screening.[10] These perspectives emphasized the need for larger datasets, standardized measurements, closer integration of material properties with printing parameters, and, ultimately, digital representations of the fabrication process.[11-13] Although this initial vision was broad, it established several themes that continue to define the field. In particular, AI is not a substitute for material characterization; rather, its value lies in using physically meaningful observations to reduce experimental burden, improve consistency, and identify interactions that are difficult to isolate manually.[14,15]

More recent reviews have shifted attention from isolated predictive tasks toward integration across the bioprinting workflow.[16] ML has been explored for quality assurance, bioink formulation, process monitoring, and translational biofabrication, while broader AI frameworks have considered how sensing, data management, and model-based decision-making could eventually enable adaptive production.[17,18] Despite these advances, recurring limitations remain. Datasets are fragmented, model validation is generally local, long-term biological endpoints are underrepresented, and model outputs are rarely incorporated into complete experimental feedback loops.[19] A substantial gap therefore persists between conceptual visions of autonomy and experimentally demonstrated capabilities.[20] Related reviews have also addressed the integration of manufacturing processes and systems, as well as the development of self-driving bioprinting laboratories.[21,22]

To complement these reviews, we focus specifically on how AI models have been implemented in experimental studies. For each representative study, we examine the research question, available data, model or learning method, and subsequent use of the model output. Importantly, we distinguish studies that only evaluated predictive performance from those in which the model was used to select a condition that was subsequently tested experimentally. We further examine the validation strategy and whether performance was evaluated using a different material, printer, or biological system. Rather than identifying a single best-performing algorithm, this review seeks to clarify the types of data and validation required before a model can reliably guide new experiments.

For this review, the bioprinting workflow is organized into four coupled domains: material, process, structure, and biology. The material domain encompasses composition, rheology, gelation, crosslinking, and cell loading.[4] The process domain includes both commanded settings and the machine state realized during fabrication.[8] The structure

domain encompasses filament geometry, pore architecture, layer alignment, local defects, channel patency, and 3D deviation from the intended design.[17] Finally, the biology domain extends from immediate cell survival to morphology, differentiation, tissue-specific function, and responses to external perturbations.[20] This four-domain organization is deliberately operational: ideally, each printed sample should be traceable across all four domains, enabling a model to learn a connected fabrication pathway rather than a collection of disconnected measurements.[8]

We further establish practical terminology to describe technological maturity. AI-assisted bioprinting refers here to bounded tasks such as regression, classification, segmentation, or parameter ranking.[16] AI-driven bioprinting describes workflows in which predictions inform material selection, parameter recommendations, quality decisions, or experimental prioritization.[18] Adaptive or closed-loop bioprinting additionally incorporates automatic sensing and bounded process adjustment, either between experiments or during printing.[17] AI-native or autonomous biofabrication represents a substantially more demanding architecture in which sample preparation, fabrication, monitoring, biological testing, model updating, and experimental planning are intentionally integrated into a continuously learning system.[20] These distinctions are important because the use of a neural network alone does not constitute autonomy.

Because some studies employ AI for multiple purposes, a single functional label may not adequately characterize the entire study. Here, terms such as prediction, classification, and monitoring describe the function performed by the model, whereas maturity level describes how the resulting model output is incorporated into the experimental workflow. A model is classified as AI-assisted when it only generates a prediction for a new sample. It is classified as AI-driven when its recommendation is used to select a condition that is subsequently tested experimentally. Adaptive or closed-loop systems extend this process by automatically using measured outcomes to modify subsequent or ongoing fabrication. Thus, a study may incorporate several AI functions, but its maturity level is determined by the highest level of workflow integration actually demonstrated. Validation and transferability are assessed separately.

The remainder of this review follows the experimental workflow. Section 2 describes the measurements used as model inputs and labels, while Section 3 examines how material, process, structural, and biological data can be integrated. Section 4 reviews studies that establish links among these data domains. Section 5 addresses inverse design and methods for selecting subsequent experiments, and Section 6 discusses the additional capabilities required for closed-loop and autonomous biofabrication. Section 7 concludes the review. This organization also distinguishes capabilities that have already been experimentally demonstrated from those that remain future objectives (Figure 1).

2. Conventional precision printing and single-modal AI approaches

The quantitative vocabulary required for contemporary AI did not originate with ML. Rather, it emerged from conventional efforts to determine whether a bioink could be deposited reproducibly while retaining a useful architecture.[23] Paxton *et al.*[24] formalized a practical two-stage assessment based on fiber formation and construct formation, together with rheological interpretation. The significance of this framework lay not in establishing a single universal threshold, but in dividing the broad concept of printability into observable behaviors that could be measured independently and subsequently used as inputs or labels for predictive models.[25] This shift from qualitative judgment toward reproducible measurement is a necessary prerequisite for reliable data-driven workflows.[26]

Ribeiro *et al.*[27] extended this logic by distinguishing collapse and fusion as separate modes of shape-fidelity failure. Collapse describes whether a filament can span an unsupported distance without excessive deflection, whereas fusion describes whether adjacent filaments maintain their intended separation after deposition. Although these outcomes may appear similar when a lattice is assessed visually, they arise from different balances among gravity, interfacial forces, viscoelasticity, extrusion history, and deposition spacing. Such distinctions are crucial for AI because a model trained on a single global quality score may obscure the physical mechanism responsible for failure and consequently recommend an inappropriate corrective action.

Biological constraints were established in parallel with geometric assessment. Ouyang *et al.*[28] examined bioink properties, printing behavior, and embryonic stem cell viability within the same experimental framework, demonstrating that conditions favorable for deposition stability are not necessarily favorable for cells. Gillispie *et al.*[29] further showed that printing parameters and cell density affect printing outcomes, emphasizing that cells are not passive components within a hydrogel. Cell loading can alter effective material behavior, modify the relationship between pressure and flow, and influence strand formation and post-print properties. These findings provide a direct rationale for treating biological composition as part of the manufacturing state rather than as metadata appended

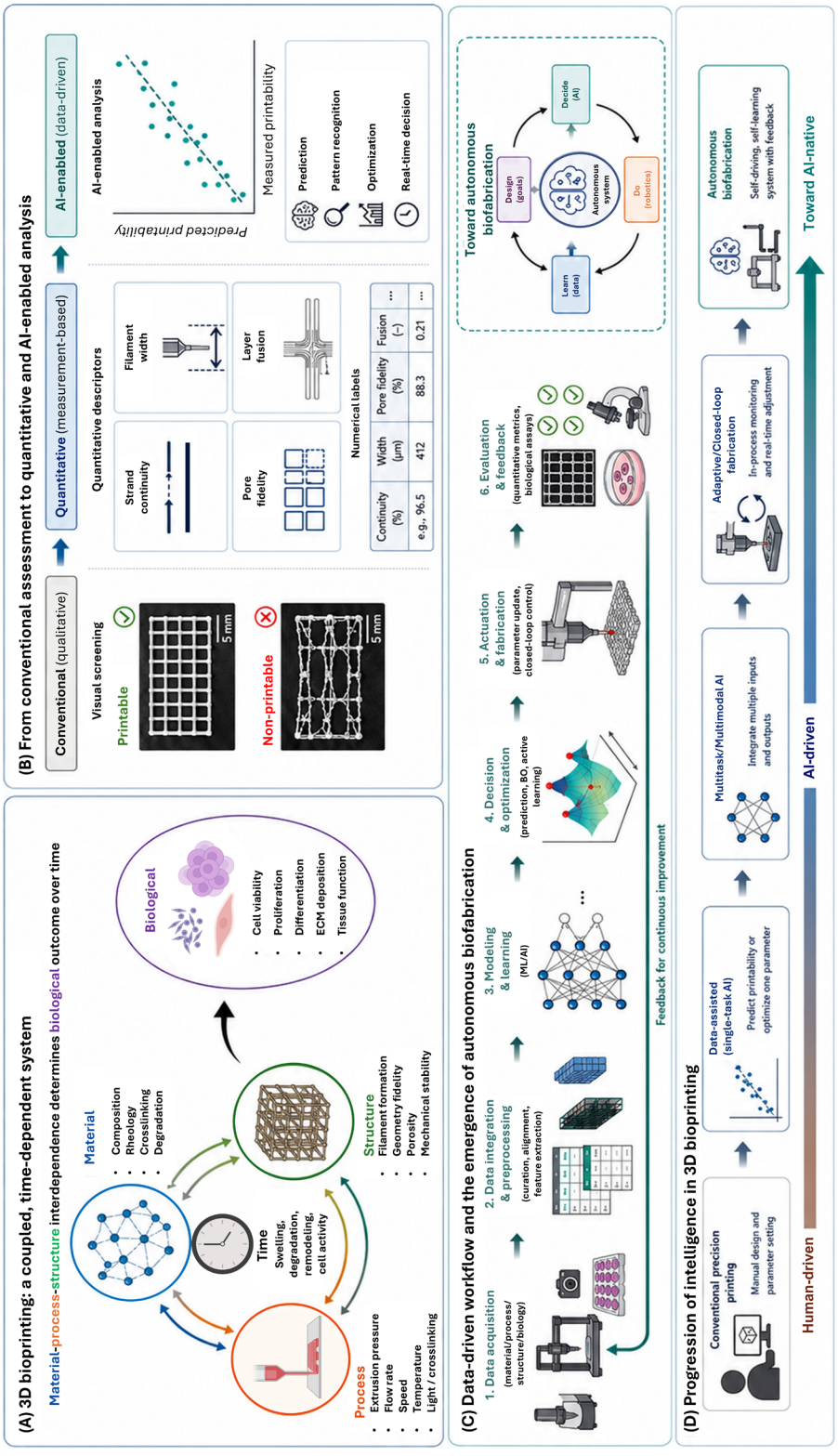


Figure 1. Conceptual overview of AI in 3D bioprinting. (A) Material, process, structure, and biology interact throughout fabrication and culture. (B) Quantitative measurements provide the basis for model training and evaluation. (C) Data acquisition, modeling, fabrication, and evaluation can be connected iteratively. (D) Increasing levels of AI use range from offline analysis to adaptive and autonomous workflows. The progression is conceptual and does not imply that all stages have already been integrated into a single operating system.
Abbreviations: AI: Artificial intelligence; BO: Bayesian optimization; ECM: Extracellular matrix; ML: Machine learning.

after printing.[30]

The dimensionality of the optimization problem increased further as fabrication strategies became more sophisticated.[31,32] Freeform reversible embedding enabled mechanically soft materials to be printed within support media, thereby expanding the range of formulations and geometries that could be fabricated.[33] Multimaterial printing of vascularized heterogeneous constructs introduced the coordinated deposition of multiple inks, sacrificial elements, and cell populations.[34] Although these approaches substantially increased design freedom, they also introduced additional coupled variables, including support-material mechanics, interfacial stability, removal conditions, channel patency, local composition, and timing between deposition steps. Such systems demonstrate why a local optimum identified for an isolated strand cannot necessarily be transferred to a complex tissue architecture.[35-38]

Rheological analysis became a key physical link between formulation and printing performance.[39-41] Flow curves characterize resistance to deformation across a range of shear rates, while storage and loss moduli provide information on elastic and viscous contributions.[42-44] Yield-like behavior, recovery after strong deformation, gelation kinetics, and temperature dependence can further indicate whether a material will begin to flow, recover after passing through a nozzle, and retain its deposited structure.[45-47] Gao *et al.*[48] systematically related gelatin alginate formulation and rheology to printing outcomes, demonstrating how these measurements can support structured optimization rather than relying on visual screening alone. More recent studies have extended this concept by investigating whether early material measurements can predict subsequent performance in specialized bioinks.[49,50]

Conventional mechanics and simulation have also provided information that later became valuable for ML.[51] Nozzle geometry, internal flow fields, and shear exposure can be investigated computationally and experimentally to estimate conditions that are difficult to measure directly.[52] Experimentally informed nozzle-design studies have demonstrated how simulation can narrow the range of candidate geometries before cell-containing experiments are conducted, while predictive modeling of formulation spaces has shown how structured experimental datasets can identify regions likely to satisfy extrusion requirements.[53] Although these approaches are not always classified as AI, they establish the same principle underlying later hybrid learning systems: expensive biological experiments can be guided by physically informative measurements and computational screening rather than conducted uniformly across the entire design space.

This progression also clarifies why early AI did not replace conventional bioprinting workflows. Instead, AI inherited their variables, experimental labels, and associated measurement biases. A printability classifier is informative only when the underlying printability assay is reproducible.[54,55] A filament-width regressor is useful only if image acquisition and segmentation are consistent.[56] Similarly, a viability predictor is trustworthy only if assay timing and biological replication are appropriate.[57] Conventional precision assessment should therefore not be viewed as a pre-AI stage that has become obsolete.[58] Instead, it remains the experimental foundation for modern prediction, monitoring, and closed-loop control.

The transition from conventional optimization to single-task AI is therefore gradual rather than binary.[59] Both approaches can use the same material and process data. The meaningful distinction emerges when a model is evaluated under genuinely unseen conditions, when its predictions are accompanied by estimates of reliability, and when its outputs inform subsequent decisions. A carefully designed regression model that prospectively identifies a useful operating region may contribute more to reproducible biofabrication than a complex neural network evaluated solely through random internal data splitting.[60-63] This distinction becomes increasingly important as the field advances toward multimodal data and adaptive workflows. The principal assessment layers established by conventional bioprinting, together with their representative measurements, contributions to AI modeling, and persistent limitations, are summarized in Table 1. Representative experimental approaches for evaluating rheology, filament formation, structural fidelity, and printability are illustrated in Figure 2, highlighting how conventional quantitative measurements provide the experimental foundation for subsequent AI-based prediction.

3. Data architecture for AI applications in bioprinting

Moving from single-task prediction toward AI-driven bioprinting requires a corresponding evolution in data architecture.[8] Rheology spreadsheets, printer logs, microscopy images, computer-aided design (CAD) files, and biological assay results are commonly stored separately and may be analyzed by different researchers at different stages of an experiment. Once the shared identity of these data is lost, multimodal modeling becomes difficult because the material state, machine event, structural feature, and biological response associated with a given construct can no longer be reliably connected. An AI-ready workflow should therefore treat each printed sample, region, strand,

Table 1. Conventional assessment layers that provide physically grounded inputs and labels for AI models

Assessment layer	Representative measurements	What contributes to AI	Persistent limitation	Ref.
Material/Rheology	Flow curve, yield-like behavior, G' and G", recovery, gelation	Physically interpretable predictors	Protocol dependence and loss of information when reduced to single values	39-50
Extrusion/Deposition	Pressure, speed, flow, nozzle, strand formation	Input–output data for process models	Commanded settings may not equal actual process state	28,29,52,53
Printed structure	Width, continuity, pore geometry, collapse, fusion, CAD deviation	Quantitative labels for regression or vision models	Often measured only in 2D and analyzed separately from biological outcomes	24,27,64,65
Biology	Viability, morphology, proliferation, phenotype, function	Application-relevant optimization targets	Delayed, noisy, cell- and assay-specific labels	28-30,57,77-85

Abbreviations: AI: Artificial intelligence; CAD: Computer-aided design.

well, or time point as a traceable experimental unit whose measurements remain linked throughout the workflow.[18]

The material domain should retain both formulation metadata and measured material responses. Relevant metadata include polymer identity and concentration, solvent or medium, crosslinker and photoinitiator content, preparation order, temperature history, time after preparation, particle or additive loading, cell type, cell density, and pre-print viability. Importantly, rheological measurements should not be prematurely reduced to a few scalar descriptors.[41] Although viscosity at a single shear rate may be sufficient for a compact model, the complete flow curve captures shear-thinning behavior that may become important when nozzle geometry or printing speed changes.[44] Likewise, fitted yield parameters, oscillatory moduli, recovery after high shear, and gelation kinetics should remain linked to the corresponding raw curves and measurement protocols.[42]

Early ML studies illustrate the importance of physically meaningful material representations. Lee *et al.*[66] used elastic modulus and yield stress to develop an ML-guided strategy for bioink design. Ruberu *et al.*[67] linked experimental printing variables to extrusion quality, while Fu *et al.*[68] used controlled experiments with Pluronic to generate parameter recommendations. Despite differences in material systems and modeling approaches, these studies follow a common principle: models are most informative when their inputs represent interpretable material or process characteristics, and their predictions narrow the experimental search space rather than merely reproduce an already established trend.

The process domain similarly requires a clear distinction between commanded settings and the physical state realized during printing. Commanded variables include pressure, volumetric flow, piston displacement, nozzle diameter, translation speed, layer height, droplet waveform, exposure time, light dose, and toolpath. Actual process behavior may deviate from these settings because of pressure lag, cartridge compliance, temperature drift, nozzle blockage, pulsation, material aging, droplet instability, or delayed extrusion. Models trained exclusively on set points implicitly assume that commanded conditions are executed perfectly. Incorporating time-aligned pressure traces, images, motor signals, or other sensor measurements instead allows the model to detect departures of the physical process from this assumption.[69]

Model architecture can also be designed to reflect hypothesized physical relationships among variables. Rheology-informed hierarchical prediction, for example, organizes formulation, rheological response, and printing resolution sequentially, reflecting a plausible pathway from material composition to printing outcome.[70] Other studies have used direct ink writing formulation data or practical scaffold-quality datasets to compare the predictive value of material features, process features, and derived descriptors.[71,72] Together, these approaches indicate that data architecture should not be determined solely by what can be conveniently exported from an instrument. Instead,

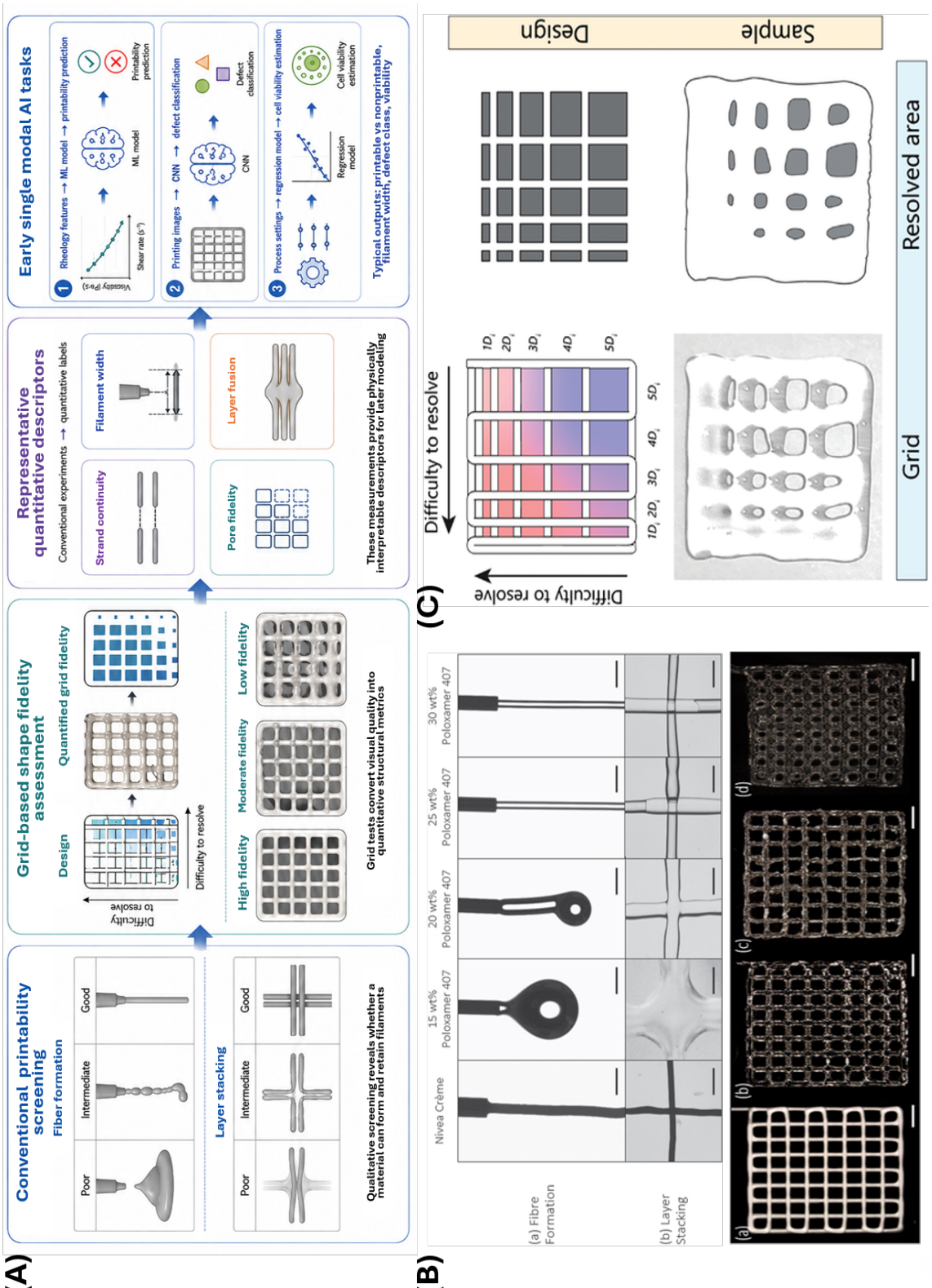


Figure 2. Conventional precision assessment and early AI applications based on individual data modalities in 3D bioprinting. (A) Schematic progression from qualitative printability screening to quantitative descriptors and AI applied to specific prediction tasks. (B) Representative fiber formation, layer stacking, and grid-printability assessments. Reprinted from Paxton *et al.*[24] (C) Grid-based design and resolved-area analysis used to quantify structural fidelity. Reprinted from Nadernezhad and Groll.[64]
Abbreviations: AI: Artificial intelligence; CNN: Convolutional neural network; ML: Machine learning.

it should preserve intermediate states expected to transmit information from experimental inputs to observed outcomes. Such an organization, however, does not itself establish causality; the proposed relationships still require experimental validation.

The structure domain can be considered an intermediate phenotype linking fabrication conditions to biological outcomes. Filament width and height, continuity, pore size and shape, layer offset, corner rounding, fusion, collapse, surface roughness, channel patency, volumetric deviation from CAD, and local stiffness arise from interactions between material properties and the printing process. At the same time, these structural characteristics define the physical environment experienced by cells. Depending on the modeling objective, structural information can be represented as hand-engineered features, segmentation masks, point clouds, image-encoder embeddings, or volumetric fields.[73,74] The appropriate representation depends on the intended use of the model. A scalar pore index may be adequate for ranking parameter combinations, whereas local process correction requires a spatially resolved defect map.

The importance of data organization becomes even more apparent as experimental datasets grow in size and heterogeneity. Studies involving multiresponse optimization with artificial neural networks, combined computational and experimental datasets for hydrogel printing, and ML-driven property prediction of hybrid bioinks demonstrate that the number of dataset entries does not necessarily reflect experimental diversity.[75-77] Hundreds of observations may still originate from only a few formulations or printing sessions. Dataset size should therefore be reported alongside the number of independent formulations, material batches, biological replicates, and machine runs.

The biological domain requires explicit organization by time scale. Immediate outcomes include cell loss, membrane damage, spatial distribution, and as-extruded viability. Short-term outcomes include attachment, morphology, proliferation, and early stress responses. Longer-term outcomes encompass differentiation, matrix production, barrier integrity, contractility, perfusion, electrophysiological behavior, tissue-specific expression, and responses to drugs.[78-83] Most AI studies emphasize immediate outcomes because rapid labels are easier to obtain. Although practical, this choice narrows the scientific objective: a model that optimizes cell survival during nozzle extrusion does not necessarily optimize subsequent functional tissue formation.[84-86]

Cross-formulation generalization and hierarchical classification illustrate how data organization can support more transferable models. Nadernezhad and Groll[64] investigated common rheological patterns across formulations containing different additives, whereas Bone *et al.*[87] decomposed high-fidelity printing into sequential decisions rather than representing all failures with a single score. Both approaches reduce reliance on formulation-specific memorization by seeking representations or decision structures that can be shared across related systems. They also demonstrate the value of interpretability in small-data biofabrication, where identifying which stage of the manufacturing pathway has failed may be as important as predicting the final outcome.

Multimodal integration, however, requires more than simply concatenating data columns. Rheological curves, images, time series, categorical descriptors, mechanical measurements, and biological assays differ in dimensionality, scale, missing-data patterns, and uncertainty. Domain-specific encoders followed by late fusion may be suitable when sufficiently large datasets are available, whereas carefully engineered features may offer greater reliability when sample sizes are limited. Regardless of representation, preventing data leakage is essential. Replicate images from the same formulation or printing run should not be distributed between training and test sets as though they were independent observations.[63] Instead, evaluation should be grouped by formulation, batch, printer, donor, or experimental day according to the intended generalization claim. Prospective validation determines how a model performs in subsequent experiments, whereas grouped holdouts assess its ability to generalize across independent groups or previously unseen conditions. The evaluation strategy should therefore reflect how the model is intended to be used. Table 2 summarizes a practical data architecture for AI-driven bioprinting by organizing the material, process, structure, and biology domains according to their raw data forms, recommended representations, and the metadata required for reproducible modeling. Figure 3 illustrates how these four domains can be integrated into a shared multimodal AI representation.

4. Linking material, process, structure, and biology using AI

Most experimental studies connect only two or three components of the material–process–structure–biology chain. We therefore organize the literature into three groups: material and rheological properties linked to printability or geometry, process monitoring linked to structural quality and correction, and material or process conditions linked to biological outcomes. This organization reflects what each model was actually designed to predict

Table 2. Recommended organization of multimodal data for AI-driven bioprinting

Domain	Raw data forms	Recommended representation	Critical metadata
Material	Composition tables and rheology curves	Raw curves plus fitted descriptors	Material lot, preparation time, temperature, cell loading
Process	Set points, logs, pressure traces, video	Time-aligned signals and event labels	Printer, nozzle, cartridge, calibration, toolpath
Structure	2D and 3D images, masks, CAD	Features, masks, embeddings, volumetric deviations	Scale, illumination, orientation, segmentation method
Biology	Images, assays, molecular and functional readouts	Temporal labels with replicate-level uncertainty	Cell type, passage number or donor, culture conditions, assay time

Abbreviations: AI: Artificial intelligence; CAD: Computer-aided design.

or control, rather than implying that every AI study operates within a fully integrated workflow.

4.1. Material and rheology to printability and geometry

Material-to-structure coupling is currently the most mature category.[8] Quantitative shape metrics provide suitable prediction targets because they can be measured rapidly and repeatedly.[50] Zhang *et al.*[65] used Hausdorff distance to compare differences between printed and target geometries, converting complex contour deviations into a reproducible numerical label. This approach is attractive because it reduces reliance on a limited set of manually selected geometric descriptors and can be extended to more complex outlines. However, a single distance value inevitably loses spatial information. For process control, both the location and type of deviation are important because similar global errors can result from under-extrusion, over-extrusion, corner rounding, or local collapse.

Studies in which model-recommended conditions are subsequently printed provide stronger experimental evidence than prediction alone. Fu *et al.*[68] tested conditions with contrasting predicted printability, whereas Ruberu *et al.*[67] repeatedly printed conditions selected during optimization. These studies demonstrate that models can guide parameter selection within the investigated material–printer combination. However, they do not establish generalization to a new material family or biological application. The scope of experimental validation must therefore be considered when comparing model performance across studies.

A further step is to identify the printing state while fabrication is still underway. Deep learning-based quality control, anomaly monitoring, and machine-assisted experimentation demonstrate three complementary strategies.[88-90] Quality-control loops can classify whether observed deposition is acceptable and use this information to support parameter adjustment.[88] Anomaly detectors can convert continuous image streams into machine-readable warnings,[89] while automated experimentation can improve the consistency and throughput of measurements used for model training.[90] Collectively, these studies demonstrate that improving the data-generation pipeline can itself be an important contribution of AI. In small-data domains, a reproducible automated measurement procedure may offer greater practical value than replacing one classifier architecture with another.

4.2. Process monitoring, structural feedback, and closed-loop correction

Real-time correction represents a stronger form of process-to-structure coupling because model outputs directly modify fabrication rather than merely characterize it. Convolutional neural network-based extrusion control has demonstrated that line quality can be identified online and translated into bounded process adjustments.[91] Computer vision-enabled control in light-based printing applies the same principle to a different physical mechanism, in which optical scattering, exposure nonuniformity, and layer formation are more important than pressure–flow dynamics.[92] Real-time computer vision for extrusion further demonstrates that the appropriate feedback signal depends on the printing modality.[93,94] These findings argue against a universal AI controller: the sensor, data representation, error metric, and corrective action need to correspond to the physical failure mode of the specific

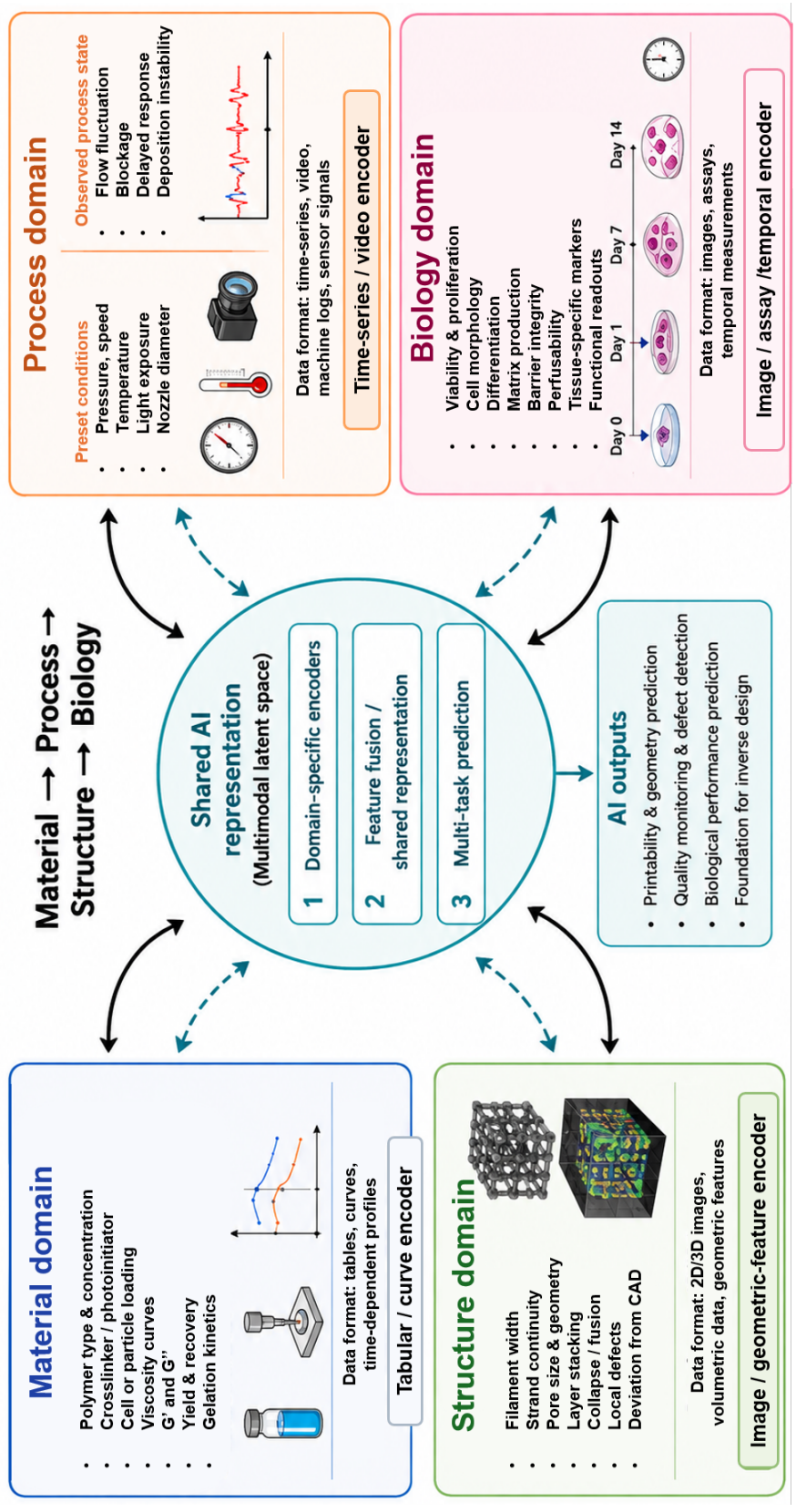


Figure 3. Multimodal representation of bioprinting as a system connecting material, process, structure, and biology. Material, process, structural, and biological data are encoded into a shared AI representation for prediction, quality monitoring, and assessment of biological performance. This shared representation is a proposed architecture for data integration and does not imply that all cited studies have implemented it.
Abbreviations: AI: Artificial intelligence; CAD: Computer-aided design.

printing process.

Bonatti *et al.*[88] and Kelly *et al.*[91] illustrate two distinct forms of feedback. Bonatti *et al.*[88] updated printing conditions between successive prints, whereas Kelly *et al.*[91] adjusted extrusion during an ongoing print. In such systems, classification accuracy alone provides an incomplete measure of performance. The more practically relevant question is whether the intervention reduces error and restores a failed or drifting process. Similarly, validation across several materials using a single device should not be interpreted as evidence of generalization to another printer or laboratory.

Structural defects can often be detected within seconds, whereas biological consequences may require days to emerge. Near-term control is therefore likely to rely primarily on rapidly available structural measurements, with delayed biological outcomes informing slower model updates. Importantly, structural measurements also need to be associated with subsequent tissue function before they can be treated as reliable biological surrogates.

4.3. Material and process conditions to biological performance

Material- and process-to-biology coupling is less mature but potentially more consequential scientifically. ML frameworks for extrusion have integrated rheological modeling, simulation, and experimental viability data to predict as-extruded cell survival from physically meaningful exposure variables.[95] Related optimization studies incorporate viability directly as an optimization objective rather than treating it solely as a final pass/fail assay.[96] Light-based bioprinting requires a different feature space because exposure dose, photoinitiator chemistry, optical attenuation, and polymerization kinetics are dominant contributors to acute cellular stress.[97] The contrast between extrusion and projection printing highlights a broader principle: biological prediction needs to reflect the mechanism of injury or stimulation associated with the relevant printing modality rather than being transferred directly from another process.

Recent studies have also moved beyond viability to model properties that define the cellular microenvironment. Neural network-based prediction of stiffness in high-cell-density constructs treats cell concentration as an active optical and mechanical variable.[98] ML-assisted spatial modulation of scaffold stiffness advances from prediction toward inverse mechanical design, while its application to a biomimetic myotendinous junction demonstrates how local process control can generate a heterogeneous interface rather than a uniform scaffold.[99,100] Compensation for cell-induced light scattering provides another important example, as the biological component itself becomes a source of manufacturing variability that can be modeled and corrected.[101]

The biological relevance of these studies nevertheless requires careful interpretation. Stiffness prediction and correction of cell-induced light scattering influence the cellular environment, but their modeled outputs remain physical quantities. Similarly, drug-response prediction in a bioprinted glioma model enables downstream biological analysis but does not, by itself, establish how printing parameters caused the observed response.[98,101,102] Biological characterization, prediction, optimization, and feedback therefore represent distinct functions and should be described separately.

Overall, material-to-structure relationships benefit from relatively accessible quantitative labels, while process monitoring has advanced to automatic correction in several systems. Biological modeling is also expanding, but relatively few studies use delayed biological outcomes to modify subsequent fabrication. A central remaining challenge is therefore to establish continuous links from material properties and machine conditions through printed structure to eventual tissue function. Figure 4 and Table 3 show representative examples of process optimization and biological analysis.

Table 3. Representative experimental studies, validation, and reported limitations

Experimental system	Model and target	Data and validation	Biological endpoint/ Experimental use	Main limitation/ Transferability	Ref.
Extrusion printing; hyaluronic acid formulations with Carbopol, Laponite, or Fmoc-FF additives; acellular.	Random forest; rheological data were used to classify grid printability.	180 formulations and 3 grids per formulation. Repeated five-fold cross-validation and out-of-bag evaluation were used.	No biological target. Post-print geometry was used for printability classification.	Tested mainly within the same experimental setup. Transfer to other printers or entirely new additive families was not shown.	64

(*Cont'd...*)

Table 3. (*Continued*)

Experimental system	Model and target	Data and validation	Biological endpoint/ Experimental use	Main limitation/ Transferability	Ref.
Extrusion printing; GelMA and GelMA/ HAMA formulations on an EnvisionTEC printer.	Bayesian optimization; printing conditions were selected using a score based on filament formation and layer stacking.	Six formulations with 4–47 printing trials per formulation. Model-selected conditions were printed and evaluated step by step.	No biological target. The model was used to recommend printing conditions that were then tested experimentally.	Tested on one printer and related materials. Transfer to other printers or material families was not shown.	67
Extrusion printing; Pluronic F127; acellular.	Support vector machine; concentration, temperature, and path height were used to predict acceptable printability.	12 training conditions. Three-fold cross-validation was followed by physical testing of conditions with high and low predicted printability.	No biological target. Line width and shape fidelity were measured, and model predictions were validated experimentally by printing.	Focused on one polymer system and printer. Repeated line measurements did not represent independent material samples.	68
Extrusion printing; 25% Pluronic F127; pneumatic and piston-based systems; acellular.	Convolutional neural network; images were classified as acceptable, under-extruded, or over-extruded, and printing settings were adjusted.	345 videos and about 30,000 frames. Internal training and testing were followed by physical monitoring and optimization experiments.	No biological target. The system monitored print quality and adjusted settings between successive prints.	Validation was mainly internal. Testing on two devices did not constitute independent validation on another printer platform or in another laboratory.	88
Extrusion printing; alginate-based training data with additional material tests; cell compatibility was also assessed.	Convolutional neural network; extrusion states were identified from real and synthetic images and used to update the extrusion factor.	512 images were used for classification evaluation, with five live print runs per model. Additional materials were tested on the same platform.	Day 0 live/dead staining was performed, but long-term cell function was not an optimization target. The model adjusted extrusion during printing.	The study focused mainly on single-layer printing, and additional-material tests were performed on the same printer platform.	91
Extrusion printing; alginate-based systems with several cell types and additional alginate/HA formulations.	Support vector modeling, fluid simulation, and cell-specific neural networks were used to predict as-extruded cell viability.	Four cell-specific datasets were used. Internal cross-validation and tests with additional composite formulations were reported.	As-extruded cell viability was the biological target. Long-term tissue function was not evaluated as an optimization target.	Separate models were used for different cell types. Transfer to a previously unseen cell type or printer was not demonstrated.	95
Light-based printing; GelMA with C2C12 myoblasts.	Optical simulation and neural networks; target images were converted into grayscale masks to compensate for light scattering.	32 physical calibration prints and 4,000 simulated mask-structure pairs were used. The learned masks were tested experimentally.	Cell loading affected light scattering, but the main target was printed geometry rather than cell function.	Much of the training data were derived from simulation. A new material or optical setup would require additional calibration and validation.	101
Light-based printing of GelMA/HAMA glioma tissue models using patient-derived samples.	Multiple regression models and weighted ensembles; gene-expression features were used to predict drug-response AUC.	The training resource included 636 cell lines and 481 compounds, while the bioprinted cohort included 23 patients. Cross-validation and additional tissue experiments were used.	Drug response was measured in short-term tissue assays, with additional characterization at later time points. The model was used for drug-response analysis, not printer control.	Most training data were not derived from bioprinted tissues, and the study did not show that printing conditions directly caused the predicted drug response.	102
Extrusion printing; 6% alginate source material and 6% alginate/4% gelatin target material; acellular.	Gaussian-process transfer regression; pressure and speed were used to predict pore-area printability.	108 source trials and 108 target trials were used. Target-material data were included during model adaptation.	No biological target. The model predicted structural fidelity and evaluated transfer between related materials.	The method still required data from the target material. Transfer to another printer or laboratory was not tested.	103

(*Cont'd...*)

Table 3. (*Continued*)

Experimental system	Model and target	Data and validation	Biological endpoint/ Experimental use	Main limitation/ Transferability	Ref.
Cellular droplet printing; GelMA/alginate systems with NIH 3T3 fibroblasts.	Decision tree, random forest, polynomial regression, multilayer perceptron, and LSTM models were compared for predicting droplet volume.	1,758 measurement instances were used with a 70/30 split, 10-fold cross-validation, model comparison, and interface demonstration.	Cell viability, proliferation, and morphology were measured over time, but were not model targets. The main prediction target was droplet volume.	Droplet-volume prediction does not directly indicate cell function, and performance on another printing platform was not tested.	104
Drop-on-demand printing of renal spheroids using induced renal epithelial cells in Matrigel.	VGG11 image-based regression and classification were used to estimate cisplatin toxicity from fluorescence images.	4,974 spheroid images were used with an 80/20 image split. No independent donor or site validation was reported.	Toxicity was predicted after spheroid maturation and drug treatment. The model was used for image-based toxicity assessment.	The labels were based on group-level dose-response results rather than direct assays of individual images, and the study did not include an automated feedback loop.	105

Abbreviations: AUC: Area under the curve; GelMA: Gelatin methacryloyl; HA: Hyaluronic acid; HAMA: Hyaluronic acid methacrylate; LSTM: Long short-term memory; VGG11: Visual Geometry Group 11.

These studies also illustrate why model accuracy alone is insufficient for evaluating practical utility. For example, a large image dataset may originate from only a small number of independent prints; a model adapted to a new material may remain restricted to the same printer; and a biological assay constitutes feedback only when its result informs a subsequent experimental step. These considerations do not diminish the value of individual studies but define the experimental range over which each model has actually been validated.

5. From forward prediction to inverse design and data-efficient experimentation

Prediction alone is not the ultimate objective of AI in bioprinting. Forward prediction estimates the outcome of a selected formulation and process.[106] The researcher specifies polymer composition, pressure, speed, nozzle, exposure conditions, or cell density, and the model predicts an outcome such as filament width, printability score, stiffness, or viability. Although this approach can reduce trial and error, candidate conditions are still selected before the model provides guidance. Inverse design reverses this sequence: the desired outcome is specified first, and the computational task is to identify regions of the material and process space capable of achieving it.[107]

In bioprinting, however, the desired outcome is rarely represented using a single scalar. A practical design target may simultaneously require filament width within a predefined tolerance, extrusion pressure below a cell-protective limit, adequate post-shear recovery, sufficient crosslinking, a defined mechanical range, and a biological response above a specified threshold. Different parameter combinations may produce similar immediate geometries while generating substantially different shear histories, transport properties, or maturation trajectories. Inverse design is therefore better formulated as constrained multi-objective decision-making than as a search for a single universal optimum.[108]

A practical inverse-design workflow begins with a surrogate model trained on structured experimental data. The surrogate approximates an expensive experimental function and may be constructed using regression, Gaussian processes, tree-based ensembles, neural networks, or hybrid models. Data-driven modeling of granular hydrogel matrices illustrates how a complex material landscape can be transformed into an experimentally navigable representation.[109] Constraint-based Bayesian optimization of bioink precursors demonstrates how probabilistic surrogates can prioritize informative conditions while excluding known infeasible regions.[110] Transfer learning addresses a complementary problem by reusing information from a related source domain when only limited data are available for the target domain.[103] Collectively, these strategies allow the modeling approach to be matched to the dominant experimental constraint, whether an extensive search space, costly labels, or a new but related material system. Importantly, studies should state whether adaptation involved data from

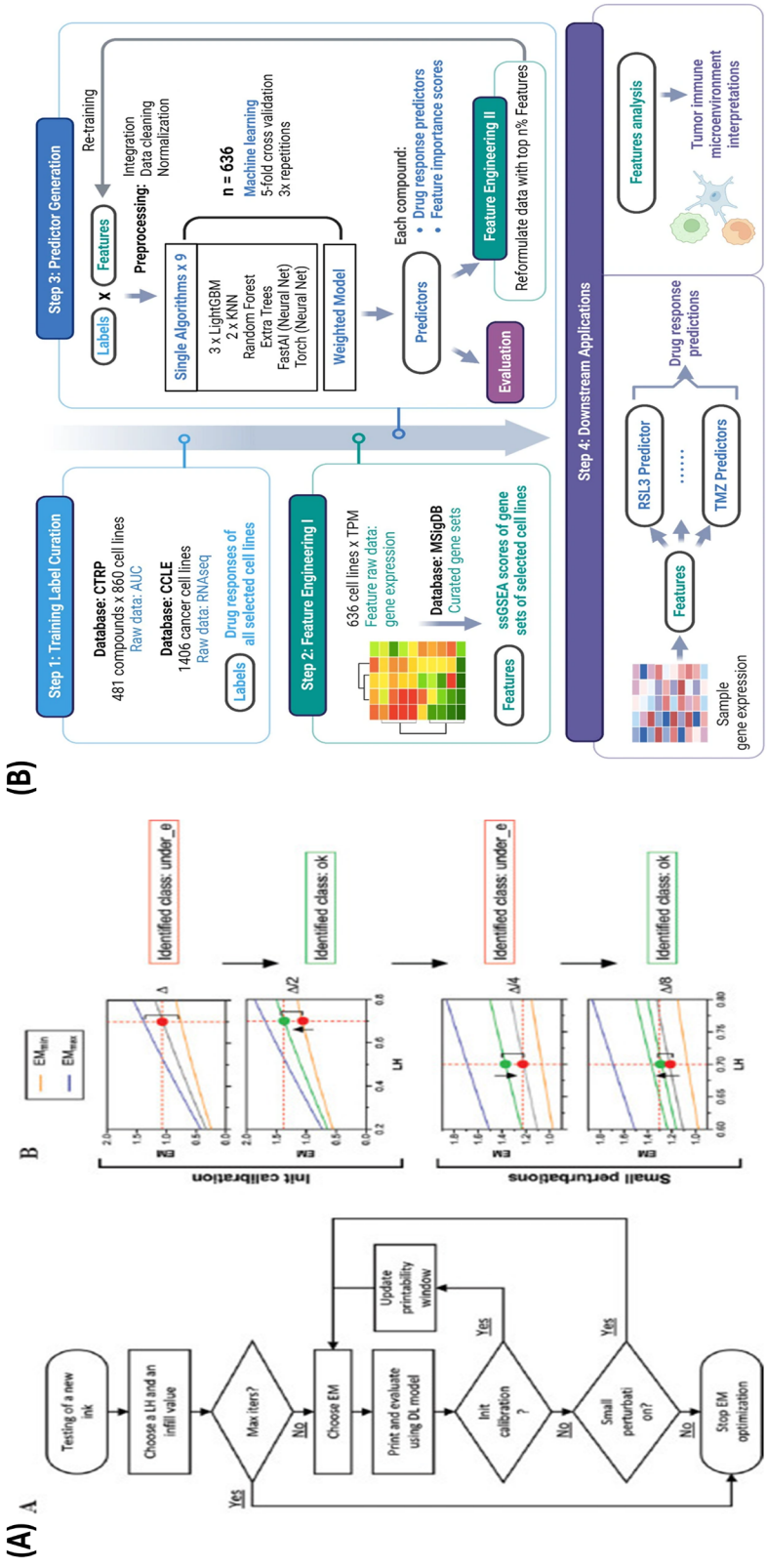


Figure 4. Representative applications of artificial intelligence (AI) in bioprinting. (A) Deep learning-based quality control and optimization of extrusion bioprinting parameters. The left panel illustrates the iterative optimization workflow, while the right panel shows changes in printing quality during parameter adjustment using layer height and extrusion multiplier. Adapted from Bonatti *et al.*[88] (B) Integration of bioprinted glioma models with ML for biological analysis. The upper panel illustrates the workflow for label generation, feature engineering, and predictor development, while the lower panel presents model evaluation and drug-response prediction results. Adapted from Tang *et al.*[102]

the new material. Improved performance after additional training on target-material data should not be interpreted as evidence of transfer to a new printer without further training.

Because individual studies differ in materials, data types, and endpoints, Table 4 provides a practical comparison rather than a ranking. It summarizes the applications, data requirements, strengths, and limitations of commonly used approaches. The first six rows represent predictive model families, whereas Bayesian optimization, active learning, transfer learning, and physics-informed or hybrid modeling are broader strategies that may incorporate one or more predictive models.[61,63,111-115]

Droplet printing provides another useful example of inverse decision-making.[116] High-throughput cellular droplet bioprinting involves interacting variables associated with waveform, droplet volume, velocity, trajectory, and cell delivery, while drop-on-demand injection requires repeated control as the reservoir state changes during operation.[104,117] ML can reduce manual waveform tuning and improve delivery consistency, but process stochasticity needs to be represented explicitly. Mean droplet size or cell count alone is insufficient when the relevant failure involves a rare satellite droplet or an empty target location. Distributional predictions and failure probabilities are therefore more informative for process design than average behavior alone.

The design loop also requires biological feedback that extends beyond terminal viability.[118] Nondestructive volumetric imaging combined with deep learning can repeatedly quantify cellular properties within 3D-bioprinted hydrogel constructs.[119] Related deep learning approaches for organoid localization, detection, tracking, and longitudinal phenotypic analysis demonstrate how image-based biological readouts can be converted into quantitative temporal labels.[120-123] AI-based nephrotoxicity analysis of bioprinted renal spheroids further demonstrates how automated interpretation can improve the throughput and objectivity of biological assays.[105] Integration of bioprinted glioma models with multiple ML algorithms extends these endpoints toward biological discovery and treatment response.[102,124,125] These studies are relevant to inverse design because downstream phenotypic analyses can provide objective functions that more closely reflect the scientific purpose of a tissue model.[126-128] However, a biological prediction model becomes useful for fabrication optimization only when its endpoint is linked to a controllable printing or culture condition, and that relationship is experimentally validated. Predicting drug response alone, for example, does not identify which printing parameter needs to be modified.

Active learning formalizes the selection of the next experiment. Rather than expanding a dataset uniformly, the algorithm selects conditions expected to provide the most useful information or reduce uncertainty efficiently. This strategy is well established in materials science and is particularly relevant to bioprinting because labeling a single condition may require preparation, sterilization, printing, imaging, and several days of culture. Complete factorial experimentation quickly becomes impractical when composition, pressure, speed, nozzle size, cell density, and crosslinking conditions are varied simultaneously. Active selection can therefore reduce experimental burden while generating data that are more informative for the intended decision.[114] Importantly, active learning and optimization have distinct objectives: active learning seeks informative experiments, whereas optimization seeks improved performance. The most informative experiment is therefore not necessarily the best-performing one. Comparisons of experimental efficiency should also use equivalent search spaces and experimental budgets, including failed prints, calibration steps, and the time required for biological measurements.

Biological experiments introduce an additional challenge because uncertainty originates from both the model and the assay. Constructs printed under nominally identical conditions can produce different viability, morphology, or expression values because of inherent biological variability. Acquisition functions should therefore distinguish epistemic uncertainty, which can be reduced by collecting additional information, from irreducible or assay-related noise.[114] In some regions of the design space, repeating an experiment may be more informative than testing a new condition. Other regions should be excluded from exploration when the predicted pressure, temperature, light dose, or chemical composition falls outside a validated biological range.

Physics-informed learning offers another means of improving data efficiency. This concept does not require every bioprinting model to take the form of a physics-informed neural network. Mechanistic knowledge can instead be incorporated through simulation-derived features, hierarchical model structures, constitutive parameters, feasibility constraints, monotonic relationships, or penalties that prevent physically impossible outputs. General physics-informed ML frameworks provide a methodological basis for integrating sparse observations with known governing relationships.[115] In bioprinting, such information can reduce the likelihood that a model learns statistical shortcuts that conflict with pressure–flow behavior, conservation principles, gelation kinetics, or established limits of cellular response.

Table 4. Comparison of commonly used AI methods and learning strategies in bioprinting

Method or strategy	Typical use	Data considerations	Strengths and limitations	Reference(s)
Linear/Regularized regression	Used for continuous outcomes when the number of numerical variables is small.	Requires independent samples that cover the range over which the model will be used.	Easy to interpret and useful as a baseline, but may fail to capture strong nonlinear relationships and does not extrapolate well.	60,103
Support vector machine/regression	Used for classification or regression with small- to medium-sized numerical datasets.	Features should be scaled, and kernel choice, hyperparameter tuning, and class balance should be considered.	Can perform well with small datasets and nonlinear decision boundaries, but results depend strongly on model configuration and tuning.	68,95,112
Tree ensembles	Used for tabular data or process data with nonlinear interactions and for feature ranking.	Requires sufficient variation across formulations or batches and adequate representation of uncommon failure cases.	Handles nonlinear relationships and can provide estimates of feature importance, but performs poorly outside the training range, and feature importance does not establish causality.	60,64,111
Multilayer perceptron	Used for nonlinear prediction of one or multiple outputs from engineered numerical features.	Requires sufficiently diverse samples relative to the number of model parameters, together with appropriate scaling and regularization.	Flexible for modeling complex relationships, but may overfit when the experimental dataset is small or narrow.	95,96,104
Convolutional/Image models	Used for image classification, segmentation, monitoring, and phenotypic analysis.	Images should represent diverse experimental conditions, and training/test splits should be made by print, video, or specimen rather than by correlated frames.	Learns image features directly, but performance can vary with lighting, image quality, correlated frames, and annotation errors. High accuracy alone does not demonstrate effective process control.	63,88,91,105
Gaussian-process surrogates	Used to model continuous responses when experiments are expensive, and the design space is limited.	Requires meaningful input variables, appropriate kernel and noise specifications, and sufficient coverage of the experimental range.	Provides both predictions and uncertainty estimates, making it suitable for small datasets, but can become computationally challenging in high-dimensional problems and remains sensitive to model assumptions.	103,113
Bayesian optimization	Used to select the next experimental condition while searching for improved performance.	Requires a surrogate model, a well-defined objective, search bounds or constraints, and results from newly tested conditions.	Can reduce the number of required experiments, but performance depends on the initial data, search range, constraints, and quality of the surrogate model.	67,96,110,113
Active learning	Used to select new samples or experiments that are expected to improve a predictive model.	Requires a candidate set, a selection criterion for informative samples, and access to new experimental labels.	Can reduce unnecessary data collection, but the most informative sample is not necessarily the highest-performing condition.	63,114
Transfer learning	Used to transfer information from one material or dataset to a related material, condition, or domain.	The source data, amount of target-domain data, adaptation method, and no-transfer baseline should be reported.	Can reduce the amount of new data required, but transfer can fail when the source and target domains differ substantially. Good performance after fine-tuning does not demonstrate generalization without target-domain data.	103
Physics-informed/ Hybrid modeling	Used to combine experimental data with simulations, physical rules, or known constraints.	Requires an appropriate physical model, information on parameter uncertainty, and experimental data for validation.	Can improve the physical consistency of predictions, but incorrect or incomplete physical assumptions can bias the model, and simulation cannot replace experimental validation.	95,101,115

Abbreviation: AI: Artificial intelligence.

Multi-objective optimization is particularly important because shape fidelity, throughput, cell protection, transport, and tissue function rarely improve simultaneously. The appropriate output may therefore be a Pareto set of nondominated solutions rather than a single nominally optimal condition.[108] Researchers can then select among these solutions according to application-specific priorities. A barrier model may emphasize uniform thickness and permeability, a screening platform may prioritize throughput and reproducibility, and a graded tissue interface may require local mechanical heterogeneity. Explicit representation of these tradeoffs is scientifically preferable to combining all objectives into a single composite score with difficult-to-justify weighting.

Robust optimization should likewise be distinguished from nominal optimization. A condition that produces the best mean outcome at a specific viscosity and temperature may fail when variation between material lots slightly alters rheology. Translational manufacturing therefore requires an operating region in which acceptable performance persists despite realistic variation in materials, machines, and biological systems. Replicate experiments and batch metadata are necessary to estimate the extent of this robust design space.[58,63] For many applications, a broad and stable operating region may be more valuable than a single highest-performing condition.

Finally, bioprinting is inherently a multi-fidelity problem. Geometric measurements can be obtained within minutes, acute viability within hours, whereas differentiation and functional readouts may require days or weeks. Waiting for the most expensive biological label after every iteration would make adaptive experimentation impractically slow. A more practical strategy is to use rapid structural or metabolic measurements as intermediate labels while incorporating slower functional assays at selected stages. When early measurements are demonstrated to predict subsequent biological behavior, optimization can proceed more rapidly while remaining connected to the long-term objective. The transition from prediction to decision-making therefore depends not only on the optimization algorithm but also on experimental scheduling and label design. Figure 5 summarizes this progression from forward prediction to inverse design through an iterative cycle of model prediction, experiment selection, fabrication, evaluation, and model updating.

6. Future perspectives toward AI-native and autonomous biofabrication

Closed-loop control and autonomous biofabrication are frequently discussed together, but they represent distinct levels of capability.[129] Automated inspection observes the process without modifying it, whereas advisory control generates recommendations that are implemented by an operator. Closed-loop control automatically adjusts bounded process variables in response to online feedback,[17] while adaptive experimentation selects subsequent experiments based on completed outcomes. A self-driving laboratory extends this concept by integrating preparation, execution, measurement, model updating, and experiment selection.[130-132] Autonomous biofabrication would further incorporate living inputs, sterile handling, maturation, and biologically informed release criteria.[22] Distinguishing these levels is essential because advances in an individual component do not establish autonomy of the entire workflow.

Current experimental systems have demonstrated several elements of adaptive fabrication, particularly rapid image-based recognition and bounded correction of geometric errors.[91] These advances establish the technical feasibility of real-time feedback but address only a fraction of the complete biofabrication workflow. Manufacturing with living systems involves operations that conventional machine control does not need to manage, including cell expansion, bioink preparation, sterile cartridge loading, prevention of cell sedimentation, media exchange, culture scheduling, biological assays, and traceable linkage of these events to the original print. For autonomous biofabrication to have a meaningful systems-level definition, automation must therefore extend beyond the printer itself.[22]

Biological delay presents one of the most difficult challenges. A manufacturing action occurs within seconds or minutes, whereas its biological consequences may emerge days later. A day-7 phenotype may reflect material preparation, acute shear exposure, local crosslinking, nutrient transport, media handling, or the culture environment. The controller therefore faces a delayed credit-assignment problem in determining which earlier decisions contributed to a later outcome. This challenge differs fundamentally from correcting filament width immediately after a camera detects over-extrusion. Biological control may require hierarchical models in which rapidly changing process states and structural surrogates are continuously updated, while slower biological measurements periodically recalibrate the long-term objective.[22] Repeated nondestructive measurements can track individual constructs over time, while separate replicates can support destructive assays. Before early structural or metabolic measurements are adopted as surrogate targets, their relationships with subsequent functional outcomes need to be established. Moreover, a delayed biological outcome constitutes true feedback only when it informs a subsequent formulation, printing

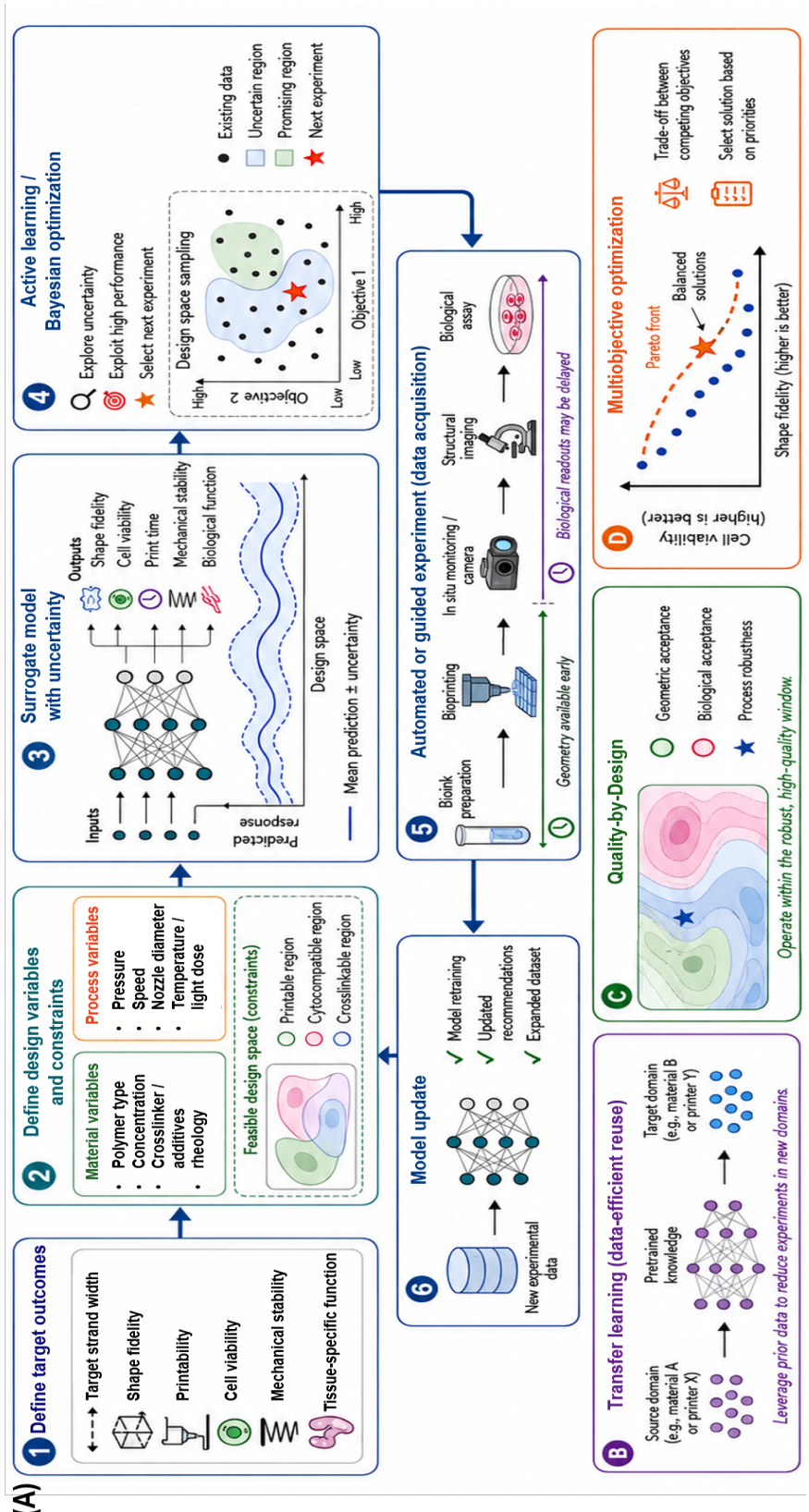


Figure 5. Example workflow for inverse design and iterative optimization in bioprinting. A target is defined, candidate designs are evaluated using a surrogate model, and new experiments are selected to update the model. Transfer learning, quality-by-design concepts, and multi-objective optimization can be incorporated depending on the application. The workflow is conceptual and does not represent an existing fully autonomous platform.

condition, or culture step.

A useful digital twin for bioprinting should consequently extend beyond a finite-element simulation or a dashboard of machine settings. It should maintain an evolving estimate of the states of the material, machine, construct, and culture. During fabrication, the twin could assimilate pressure signals, image streams, temperature measurements, toolpath information, and model-based estimates of local stress. After fabrication, structural imaging, mechanical measurements, and biological assays could update the estimated state of the construct. Predictions of geometry, local properties, and biological trajectories could then be revised as new observations become available. The utility of such a digital twin depends primarily on synchronization rather than visual sophistication.[133]

Achieving this synchronization requires rigorous identity management. The computational representation must retain information on the material lot, preparation batch, cartridge, nozzle, cell population, toolpath, print region, and culture vessel associated with each observation. Without these links, the digital state cannot be reliably reconciled with the physical experiment after events such as cartridge replacement or culture transfer. Sample identity and data provenance are therefore fundamental enabling technologies for autonomy.[133] They also improve model auditability by allowing unexpected predictions to be traced to the corresponding material, process, and biological history.

Benchmarking is another prerequisite for reliable autonomy. Community datasets should include raw and processed rheological data, printer commands, machine logs, synchronized videos, target geometries, segmentation masks, biological labels, and batch metadata. Evaluation splits should correspond to the intended generalization claim. Random sample splits primarily assess interpolation, leave-formulation-out evaluation assesses material generalization, leave-printer-out evaluation assesses platform transfer, and independent-site evaluation assesses reproducibility across laboratories.[58] Prospective experiments provide more direct evidence of decision-support capability when model-selected actions are implemented and evaluated in subsequent fabrication experiments.[62,134] Evaluation metrics should also address calibration, failure detection, and abstention behavior rather than relying solely on R^2, root mean square error, or classification accuracy. Prospective testing, however, does not replace evaluation on data held out by material, printer, or laboratory when transfer to those conditions is claimed. For control studies, authors should report the consequences of model-initiated process adjustments and whether failed or drifting prints were successfully recovered. For biological optimization, improvement should ultimately be demonstrated in the biological function itself rather than only in a correlated geometric measure.

Human supervision will remain important as automation increases. Trustworthy autonomy requires explicit operating limits and the ability to defer decisions when uncertainty is sufficiently high.[130] Safety boundaries can prevent pressures, temperatures, light doses, or material concentrations from exceeding validated ranges regardless of model confidence. Out-of-distribution detection can identify materials or image states that differ substantially from the training domain. The controller can then stop the process, request an additional measurement, or defer the decision to an operator. Such mechanisms improve both safety and scientific transparency by treating uncertainty as actionable information rather than converting it into an unjustified decision.

Sterile automation introduces additional engineering constraints. Robotic systems must handle materials whose rheological properties evolve with time and temperature while maintaining sterility. Cell reservoirs may require controlled mixing to maintain uniform cell concentrations, while automated nozzle replacement must preserve spatial calibration. Imaging and assay modules need to interact with culture vessels without compromising sterile conditions. Waste handling, decontamination, and recovery from failed dispensing events also need to be integrated. These requirements illustrate why autonomous biofabrication is not primarily an algorithmic problem. Rather, it is a systems-engineering challenge integrating robotics, sensing, process control, data infrastructure, biomaterials science, and cell culture.[22]

Self-driving bioprinting laboratories have now been explicitly proposed as a design–build–test–learn architecture integrating automated cell culture, bioink preparation, printing, maturation, monitoring, and AI-guided experimental planning.[22] This long-term concept emphasizes that the printer represents only one component of the overall loop. It also supports staged implementation, in which reliable modules are progressively connected. For example, a laboratory can standardize sample tracking before automating bioink preparation, automate imaging before introducing autonomous experiment selection, and validate an individual closed feedback loop before integrating multiple loops.[130-132]

To distinguish these levels of AI integration, we propose a five-level scheme (Table 5). Level 0 represents conventional manual optimization. Level 1 encompasses offline prediction or classification without model-selected experimental action. Level 2 requires a model

recommendation to be implemented and evaluated experimentally. Level 3 adds automatic adjustment based on measured feedback; this adjustment may occur between successive prints or during an ongoing print, with both forms assigned the same maturity level. Level 4 represents a broader autonomous system in which preparation, printing, monitoring, biological testing, model updating, and selection of subsequent experiments are integrated. These levels describe how AI is incorporated into the experimental workflow and are independent of the extent of external validation.

Near-term priorities should therefore emphasize trustworthy integration rather than maximum automation.[135] Standardized metadata, independent validation, uncertainty-aware recommendations, nondestructive biological monitoring, robust operating windows, and transfer across materials and printers can improve current AI systems while simultaneously establishing the infrastructure required for future autonomy.[136] Progress is likely to be cumulative: each module should first demonstrate improved reproducibility or decision quality within a defined scope, after which interfaces among modules can be standardized and validated.[137] Autonomy becomes scientifically meaningful only when the integrated system performs reliably under sources of variation that were not encountered during model development.[138]

Table 5. Proposed maturity framework for AI integration in 3D bioprinting

Level	Designation	Required capability
0	Conventional	Manual design, printing, inspection, and repetition.
1	AI-assisted	Offline prediction or classification; the model does not select an experimental action.
2	AI-driven	A model recommendation is implemented and evaluated experimentally.
3	Adaptive or closed-loop	Measured feedback triggers an automatic adjustment either between prints or during printing.
4	Autonomous biofabrication	Preparation, printing, monitoring, biological testing, model updating, and selection of the next experiment are linked in one automated workflow.

Abbreviation: AI: Artificial intelligence.

7. Conclusion

The experimental literature demonstrates that AI is already a substantive enabling technology in 3D bioprinting. AI models can relate material properties to printability, predict resolution and cell survival, automate image-based quality assessment, recommend process parameters, compensate for selected process disturbances, transfer information between related domains, optimize droplet delivery, and extract biological phenotypes from printed tissue models. These capabilities demonstrate that AI has progressed beyond conceptual applications and is beginning to influence how bioprinting experiments are designed, conducted, and interpreted.

Despite this progress, most published models remain specific to a particular material family, printer, imaging setup, or biological assay. Cross-laboratory validation remains uncommon, and long-term tissue function is more often evaluated after optimization than incorporated directly into the optimization process. Current bioprinting therefore remains predominantly AI-assisted, although AI-driven and adaptive applications are increasing. Importantly, greater automation alone does not demonstrate broader transferability or improved tissue function.

The next step is to integrate measurements that are currently treated separately. Material properties need to be linked to the actual machine state, machine state to local 3D structure, and structure to subsequent biological function. Inverse design, active learning, constrained optimization, transfer learning, physics-informed reasoning, and measurements acquired across different time scales can contribute to this integration. However, their utility ultimately depends on the quality, traceability, and representativeness of the experiments used for model training and validation. Comparing the data requirements, intended functions, and validation domains of different

methods is therefore more informative than identifying a single algorithm as a general solution.

Autonomous biofabrication is best regarded as a long-term objective rather than a label for any system incorporating a neural network or automated actuator. Progress will potentially depend on progressively connecting reliable components: reproducible measurements, traceable samples, prospective validation, uncertainty estimates, robust process windows, automated measurements, and biologically meaningful feedback. Ultimately, the value of AI in bioprinting will depend on whether it can improve decisions about what to fabricate, how to fabricate it, how to evaluate it over time, and which experiment to perform next.

Acknowledgments

None.

Funding

This work was supported by the National Research Foundation of Korea (NRF) grant funded by the Korean government (MSIT) (No. RS-2024-00423107, RS-2025–23524743, and RS-2026-25516708).

Conflict of interest

The authors declare they have no competing interests.

Author contributions

Conceptualization: Jooyoung Lee, Hyungseok Lee
Supervision: Hyungseok Lee
Visualization: Jooyoung Lee
Writing–original draft: Jooyoung Lee
Writing–review & editing: Jooyoung Lee, Hyungseok Lee

Ethics approval and consent to participate

Not applicable.

Consent for publication

Not applicable.

Availability of data

Not applicable.

AI tools statement

None.

References

1. Groll J, Boland T, Blunk T, *et al*. Biofabrication: reappraising the definition of an evolving field. *Biofabrication*. 2016;8(1):013001.

doi: 10.1088/1758-5090/8/1/013001

2. Zhang Y, Yue K, Aleman J, *et al*. 3D bioprinting for tissue and organ fabrication. *Ann Biomed Eng*. 2017;45(1):148-163.

doi: 10.1007/s10439-016-1612-8

3. Murphy S, De Coppi P, Atala A. Opportunities and challenges of translational 3D bioprinting. *Nat Biomed Eng*. 2020;4(4):370-380.

doi: 10.1038/s41551-019-0471-7

4. Sun W, Starly B, Daly A, *et al*. The bioprinting roadmap. *Biofabrication*. 2020;12(2):022002.

doi: 10.1088/1758-5090/ab5158

5. Schwab A, Levato R, D'Este M, Piluso S, Eglin D, Malda J. Printability and shape fidelity of bioinks in 3D bioprinting. *Chem Rev*. 2020;120(19):11028-11055.

doi: 10.1021/acs.chemrev.0c00084

6. Gillispie G, Prim P, Copus J, *et al*. Assessment methodologies for extrusion-based bioink printability. *Biofabrication*. 2020;12(2):022003.

doi: 10.1088/1758-5090/ab6f0d

7. Resende MAA, Rigo ECS, Vercik A. Printability of bioinks: a consolidated definition for additive manufacturing. *ACS Omega*. 2025;10(48):58110-58122.

doi: 10.1021/acsomega.5c00727

8. Lee JS, Cha JH, Kim BS. Artificial intelligence in 3D bioprinting and biofabrication: a validation-stringency assessment. *Biofabrication*. 2026;18(3):032003.

doi: 10.1088/1758-5090/ae7b07

9. Al-Kharusi G, Dunne NJ, Little S, Levingstone TJ. The role of machine learning and design of experiments in the advancement of biomaterial and tissue engineering research. *Bioengineering (Basel)*. 2022;9(10):561.

doi: 10.3390/bioengineering9100561

10. Yu C, Jiang J. A perspective on using machine learning in 3D bioprinting. *Int J Bioprint*. 2020;6(1):253.

doi: 10.18063/ijb.v6i1.253

11. Sun J, Yao K, An J, Jing L, Huang K, Huang D. Machine learning and 3D bioprinting. *Int J Bioprint*. 2023;9(4):717.

doi: 10.18063/ijb.717

12. Freeman S, Calabro S, Williams R, Jin S, Ye K. Bioink formulation and machine learning-empowered bioprinting optimization. *Front Bioeng Biotechnol*. 2022;10:913579.

doi: 10.3389/fbioe.2022.913579

13. Ng WL, Goh GL, Goh GD, Ten JSJ, Yeong WY. Progress and opportunities for machine learning in materials and processes of additive manufacturing. *Adv Mater*. 2024;36(34):e2310006.

doi: 10.1002/adma.202310006

14. Ning H, Zhou T, Joo SW. Machine learning boosts three-dimensional bioprinting. *Int J Bioprint*. 2023;9(4):739.

doi: 10.18063/ijb.739

15. Filippi M, Mekkattu M, Katzschmann RK. Sustainable biofabrication: from bioprinting to AI-driven predictive methods. *Trends Biotechnol*. 2025;43(2):290-303.

doi: 10.1016/j.tibtech.2024.07.002

16. Chen H, Zhang B, Huang J. Recent advances and applications of artificial intelligence in 3D bioprinting. *Biophys Rev*. 2024;5(3):031301.

doi: 10.1063/5.0190208

17. Bonatti A, Vozzi G, De Maria C. Enhancing quality control in bioprinting through machine learning. *Biofabrication*. 2024;16(2):022001.

doi: 10.1088/1758-5090/ad2189

18. Zhou C, Liu C, Liao Z, Pang Y, Sun W. AI for biofabrication. *Biofabrication*. 2025;17(1):012004.

doi: 10.1088/1758-5090/ad8966

19. Zhang Z, Zhou X, Fang Y, Xiong Z, Zhang T. AI-driven 3D bioprinting for regenerative medicine: from bench to bedside. *Bioact Mater*. 2025;45:201-230.

doi: 10.1016/j.bioactmat.2024.11.021

20. Robazzi J, Derman I, Gupta D, *et al*. The synergy of artificial intelligence and 3D bioprinting: unlocking new frontiers in precision and tissue fabrication. *Adv Funct Mater*. 2026;36(1):e09530.

doi: 10.1002/adfm.202509530

21. Ramesh S, Deep A, Tamayol A, Kamaraj A, Mahajan C, Madihally S. Advancing 3D bioprinting through machine learning and artificial intelligence. *Bioprinting*. 2024;38:e00331.

doi: 10.1016/j.bprint.2024.e00331

22. Liu S, Kaur N, Song D, Moses J, Ozbolat I. Self-driving bioprinting laboratories. *Biofabrication*. 2026;18(1):013001.

doi: 10.1088/1758-5090/ae3645

23. Naghieh S, Chen X. Printability—a key issue in extrusion-based bioprinting. *J Pharm Anal*. 2021;11(5):564-579.

doi: 10.1016/j.jpha.2021.02.001

24. Paxton N, Smolan W, Böck T, Melchels F, Groll J, Jungst T. Proposal to assess printability of bioinks for extrusion-based bioprinting and evaluation of rheological properties governing bioprintability. *Biofabrication*. 2017;9(4):044107.

doi: 10.1088/1758-5090/aa8dd8

25. Theus A, Ning L, Hwang B, *et al*. Bioprintability: physiomechanical and biological requirements of materials for 3D bioprinting processes. *Polymers (Basel)*. 2020;12(10):2262.

doi: 10.3390/polym12102262

26. Strauß S, Grijalva Garces D, Hubbuch J. Analytics in extrusion-based bioprinting: standardized methods improving quantification and comparability of the performance of bioinks. *Polymers (Basel)*. 2023;15(8):1829.

doi: 10.3390/polym15081829

27. Ribeiro A, Blokzijl M, Levato R, *et al*. Assessing bioink shape fidelity to aid material development in 3D bioprinting. *Biofabrication*. 2018;10(1):014102.

doi: 10.1088/1758-5090/aa90e2

28. Ouyang L, Yao R, Zhao Y, Sun W. Effect of bioink properties on printability and cell viability for 3D bioplotting of embryonic stem cells. *Biofabrication*. 2016;8(3):035020.

doi: 10.1088/1758-5090/8/3/035020

29. Gillispie GJ, Han A, Uzun-Per M, *et al*. The influence of printing parameters and cell density on bioink printing outcomes. *Tissue Eng Part A*. 2020;26(23-24):1349-1358.

doi: 10.1089/ten.TEA.2020.0210

30. Malekpour A, Chen X. Printability and cell viability in extrusion-based bioprinting from experimental, computational, and machine learning views. *J Funct Biomater*. 2022;13(2):40.

doi: 10.3390/jfb13020040

31. Derman I, Kim M, Dogan Sarikaya M. Unconventional bioprinting modalities for advanced tissue biofabrication. *Biomaterials*. 2026;326:123704.

doi: 10.1016/j.biomaterials.2025.123704

32. Cui X, Li J, Hartanto Y. Advances in extrusion 3D bioprinting: a focus on multicomponent hydrogel-based bioinks. *Adv Healthc Mater*. 2020;9(15):e1901648.

doi: 10.1002/adhm.201901648

33. Hinton T, Jallerat Q, Palchesko R, *et al*. Three-dimensional printing of complex biological structures by freeform reversible embedding of suspended hydrogels. *Sci Adv*. 2015;1(9):e1500758.

doi: 10.1126/sciadv.1500758

34. Kolesky D, Truby R, Gladman A, Busbee T, Homan K, Lewis J. 3D bioprinting of vascularized, heterogeneous cell-laden tissue constructs. *Adv Mater*. 2014;26(19):3124-3130.

doi: 10.1002/adma.201305506

35. Michel R, Auzély-Velty R. Hydrogel-colloid composite bioinks for targeted tissue-printing. *Biomacromolecules*. 2020;21(8):2949-2965.

doi: 10.1021/acs.biomac.0c00305

36. Vrana N, Gupta S, Mitra K. From 3D printing to 3D bioprinting: the material properties of polymeric material

and its derived bioink for achieving tissue specific architectures. *Cell Tissue Bank*. 2022;23(3):417-440.

doi: 10.1007/s10561-021-09975-z

37. Papaioannou T, Manolesou D, Dimakakos E, Tsoucalas G, Vavuranakis M, Tousoulis D. 3D bioprinting methods and techniques: applications on artificial blood vessel fabrication. *Acta Cardiol Sin*. 2019;35(3):284-289.

doi: 10.6515/ACS.201905_35(3).20181115A

38. Li X, Zheng F, Wang X. Biomaterial inks for extrusion-based 3D bioprinting: property, classification, modification, and selection. *Int J Bioprint*. 2023;9(2):649.

doi: 10.18063/ijb.v9i2.649

39. García-Villén F, Ruiz-Alonso S, Lafuente-Merchan M. Clay minerals as bioink ingredients for 3D printing and 3D bioprinting: application in tissue engineering and regenerative medicine. *Pharmaceutics*. 2021;13(11):1806.

doi: 10.3390/pharmaceutics13111806

40. Lee S, Gillispie G, Prim P, Lee S. Physical and chemical factors influencing the printability of hydrogel-based extrusion bioinks. *Chem Rev*. 2020;120(19):10834-10886.

doi: 10.1021/acs.chemrev.0c00015

41. Hölzl K, Lin S, Tytgat L, Van Vlierberghe S, Gu L, Ovsianikov A. Bioink properties before, during and after 3D bioprinting. *Biofabrication*. 2016;8(3):032002.

doi: 10.1088/1758-5090/8/3/032002

42. Cooke M, Rosenzweig D. The rheology of direct and suspended extrusion bioprinting. *APL Bioeng*. 2021;5(1):011502.

doi: 10.1063/5.0031475

43. Lan X, Adesida A, Boluk Y. Rheological and viscoelastic properties of collagens and their role in bioprinting by micro-extrusion. *Biomed Mater*. 2022;17(6):062005.

doi: 10.1088/1748-605X/ac9b06

44. Amorim P, d'Ávila M, Anand R, Moldenaers P, Van Puyvelde P, Bloemen V. Insights on shear rheology of inks for extrusion-based 3D bioprinting. *Bioprinting*. 2021;22:e00129.

doi: 10.1016/j.bprint.2021.e00129

45. Ouyang L. Pushing the rheological and mechanical boundaries of extrusion-based 3D bioprinting. *Trends Biotechnol*. 2022;40(7):891-902.

doi: 10.1016/j.tibtech.2022.01.001

46. Das S, Jegadeesan J, Basu B. Gelatin methacryloyl (GelMA)-based biomaterial inks: process science for 3D/4D printing and current status. *Biomacromolecules*. 2024;25(4):2156-2221.

doi: 10.1021/acs.biomac.3c01271

47. Elango J, Zamora-Ledezma C. Rheological, structural, and biological trade-offs in bioink design for 3D bioprinting. *Gels*. 2025;11(8):659.

doi: 10.3390/gels11080659

48. Gao T, Gillispie G, Copus J, *et al*. Optimization of gelatin-alginate composite bioink printability using rheological parameters: a systematic approach. *Biofabrication*. 2018;10(3):034106.

doi: 10.1088/1758-5090/aacdc7

49. da Silva V, Yu B, Willerth S. Early-stage material properties as predictors of neural bioink performance during extrusion 3D bioprinting. *Biofabrication*. 2026;18(2):025002.

doi: 10.1088/1758-5090/ae46e2

50. Sarah R, Rohauer R, Schimmelpfennig K, Limon S, Lewis C, Habib A. Data-driven optimization of bioink formulations for extrusion-based bioprinting: a predictive modeling approach. *J Manuf Sci Eng*. 2025;147(10):101001.

doi: 10.1115/1.4069041

51. Chen XB, Anvari-Yazdi AF, Duan X, *et al*. Biomaterials/bioinks and extrusion bioprinting. *Bioact Mater*. 2023;28:511-536.

doi: 10.1016/j.bioactmat.2023.06.006

52. Gharraei R, Bergstrom D, Chen X. Extrusion bioprinting from a fluid mechanics perspective. *Int J Bioprint*. 2024;10(6):3973.

doi: 10.36922/ijb.3973

53. Reina-Romo E, Mandal S, Amorim P, Bloemen V, Ferraris E, Geris L. Towards the experimentally-informed in silico nozzle design optimization for extrusion-based bioprinting of shear-thinning hydrogels. *Front Bioeng Biotechnol*. 2021;9:701778.

doi: 10.3389/fbioe.2021.701778

54. Kyle S, Jessop Z, Al-Sabah A, Whitaker I. "Printability" of candidate biomaterials for extrusion based 3D printing: state-of-the-art. *Adv Healthc Mater*. 2017;6(16):e1700264.

doi: 10.1002/adhm.201700264

55. Fu Z, Naghieh S, Xu C, Wang C, Sun W, Chen X. Printability in extrusion bioprinting. *Biofabrication*. 2021;13(3):033001.

doi: 10.1088/1758-5090/abe7ab

56. Stringer C, Wang T, Michaelos M, Pachitariu M. Cellpose: a generalist algorithm for cellular segmentation. *Nat Methods*. 2021;18(1):100-106.

doi: 10.1038/s41592-020-01018-x

57. Wang J, Cui Z, Maniruzzaman M. Bioprinting: a focus on improving bioink printability and cell performance based on different process parameters. *Int J Pharm*. 2023;640:123020.

doi: 10.1016/j.ijpharm.2023.123020

58. Grijalva Garces D, Strauss S, Gretzinger S. On the

reproducibility of extrusion-based bioprinting: round robin study on standardization in the field. *Biofabrication*. 2024;16(1):015002.

doi: 10.1088/1758-5090/acfe3b

59. Yu J, Yao D, Wang L, Xu M. Machine learning in predicting and optimizing polymer printability for 3D bioprinting. *Polymers (Basel)*. 2025;17(13):1873.

doi: 10.3390/polym17131873

60. Conev A, Litsa EE, Perez MR, Diba M, Mikos AG, Kavraki LE. Machine learning-guided three-dimensional printing of tissue engineering scaffolds. *Tissue Eng Part A*. 2020;26(23-24):1359-1368.

doi: 10.1089/ten.tea.2020.0191

61. Varoquaux G, Cheplygina V. Machine learning for medical imaging: methodological failures and recommendations for the future. *NPJ Digit Med*. 2022;5:48.

doi: 10.1038/s41746-022-00592-y

62. Dabbagh SR, Ozcan O, Tasoglu S. Machine learning-enabled optimization of extrusion-based 3D printing. *Methods*. 2022;206:27-40.

doi: 10.1016/j.ymeth.2022.08.002

63. Kapoor S, Narayanan A. Leakage and the reproducibility crisis in machine-learning-based science. *Patterns*. 2023;4(9):100804.

doi: 10.1016/j.patter.2023.100804

64. Nadernezhad A, Groll J. Machine learning reveals a general understanding of printability in formulations based on rheology additives. *Adv Sci (Weinh)*. 2022;9(29):2202638.

doi: 10.1002/advs.202202638

65. Zhang C, Elvitigala K, Sakai S. AI-powered printability evaluation framework for 3D bioprinting using Hausdorff distance metrics. *Biofabrication*. 2026;18(1):015015.

doi: 10.1088/1758-5090/ae288c

66. Lee J, Oh SJ, An SH, Kim WD, Kim SH. Machine learning-based design strategy for 3D printable bioink: elastic modulus and yield stress determine printability. *Biofabrication*. 2020;12(3):035018.

doi: 10.1088/1758-5090/ab8707

67. Ruberu K, Senadeera M, Rana S, *et al*. Coupling machine learning with 3D bioprinting to fast track optimisation of extrusion printing. *Appl Mater Today*. 2021;22:100914.

doi: 10.1016/j.apmt.2020.100914

68. Fu Z, Angeline V, Sun W. Evaluation of printing parameters on 3D extrusion printing of Pluronic hydrogels and machine learning guided parameter recommendation. *Int J Bioprint*. 2021;7(4):179-189.

doi: 10.18063/ijb.v7i4.434

69. Zanderigo G, Afghah F, Colosimo BM, Raman R. Modular and AI-driven in situ monitoring platform for real-time process analysis in embedded bioprinting. *Device*. 2025;3(11):100927.

doi: 10.1016/j.device.2025.100927

70. Oh D, Shirzad M, Kim M, Chung E, Nam S. Rheology-informed hierarchical machine learning model for the prediction of printing resolution in extrusion-based bioprinting. *Int J Bioprint*. 2023;9(6):1280.

doi: 10.36922/ijb.1280

71. Chen H, Liu Y, Balabani S, Hirayama R, Huang J. Machine learning in predicting printable biomaterial formulations for direct ink writing. *Research (Wash D C)*. 2023;6:0197.

doi: 10.34133/research.0197

72. Rafieyan S, Ansari E, Vasheghani-Farahani E. A practical machine learning approach for predicting the quality of 3D (bio)printed scaffolds. *Biofabrication*. 2024;16(4):045014.

doi: 10.1088/1758-5090/ad6374

73. Yao K, Sun J, Huang K, *et al*. Analyzing cell-scaffold interaction through unsupervised 3D nuclei segmentation. *Int J Bioprint*. 2022;8(1):495.

doi: 10.18063/ijb.v8i1.495

74. Balters L, Reichl S. A design of experiment to evaluate the printability for bioprinting by using deep learning image similarity. *J Biomed Mater Res A*. 2025;113(7):e37961.

doi: 10.1002/jbm.a.37961

75. Qavi I, Halder S, Tan G. Optimization of printability of bioinks with multi-response optimization and artificial neural networks. *Prog Addit Manuf*. 2025;10(5):3573-3598.

doi: 10.1007/s40964-024-00828-1

76. Bediaga-Bañeres H, Moreno-Benítez I, Arrasate S. Artificial intelligence-driven modeling for hydrogel three-dimensional printing: computational and experimental cases of study. *Polymers (Basel)*. 2025;17(1):121.

doi: 10.3390/polym17010121

77. Sarah R, Schimmelpfennig K, Rohauer R, Lewis C, Limon S, Habib A. Characterization and machine learning-driven property prediction of a novel hybrid hydrogel bioink considering extrusion-based 3D bioprinting. *Gels*. 2025;11(1):45.

doi: 10.3390/gels11010045

78. Zhang D, Huerta-López C, Heilshorn S. Organoid bioprinting to pattern the matrix microenvironment. *Curr Opin Biomed Eng*. 2025;35:100607.

doi: 10.1016/j.cobme.2025.100607

79. Kang D, Park J, Kim W, *et al*. All-inkjet-printed 3D alveolar barrier model with physiologically relevant microarchitecture. *Adv Sci (Weinh)*. 2021;8(10):2004990.

doi: 10.1002/advs.202004990

80. Zhang X, Zhao G, Ma T, Simmons C, Santerre J. A critical review on advances and challenges of bioprinted cardiac patches. *Acta Biomater*. 2024;189:1-24.

doi: 10.1016/j.actbio.2024.09.056

81. Revokatova D, Bikmulina P, Heydari Z, *et al*. Getting blood out of a stone: vascularization via spheroids and organoids in 3D bioprinting. *Cells*. 2025;14(9):665.

doi: 10.3390/cells14090665

82. Kupfer ME, Lin WH, Ravikumar V, *et al*. In situ expansion, differentiation, and electromechanical coupling of human cardiac muscle in a 3D bioprinted, chambered organoid. *Circ Res*. 2020;127(2):207-224.

doi: 10.1161/CIRCRESAHA.119.316155

83. Hwang H, Liu R, Maxwell JT, Yang J, Xu C. Machine learning identifies abnormal Ca2+ transients in human induced pluripotent stem cell-derived cardiomyocytes. *Sci Rep*. 2020;10:16977.

doi: 10.1038/s41598-020-73801-x

84. Huang M, Christakopoulos F, Roth J, Heilshorn S. Organoid bioprinting: from cells to functional tissues. *Nat Rev Bioeng*. 2025;3(2):126-142.

doi: 10.1038/s44222-024-00268-0

85. Ho YH, Liao Y, Liao L, Mao T, Guan Y, Xu R. Advances of cell printing technology in organoid engineering. *Tissue Eng Part B Rev*. 2026;32(5):348-358.

doi: 10.1089/ten.TEB.2025.0048

86. Li Z, Chen L, Wu J. A review of 3D bioprinting for organoids. *Med Rev (2021)*. 2025;5(4):318-338.

doi: 10.1515/mr-2024-0089

87. Bone J, Childs C, Menon A. Hierarchical machine learning for high-fidelity 3D printed biopolymers. *ACS Biomater Sci Eng*. 2020;6(12):7021-7031.

doi: 10.1021/acsbiomaterials.0c00755

88. Bonatti A, Vozzi G, Chua C, De Maria C. A deep learning quality control loop of the extrusion-based bioprinting process. *Int J Bioprint*. 2022;8(4):620.

doi: 10.18063/ijb.v8i4.620

89. Jin Z, Zhang Z, Shao X, Gu G. Monitoring anomalies in 3D bioprinting with deep neural networks. *ACS Biomater Sci Eng*. 2023;9(7):3945-3952.

doi: 10.1021/acsbiomaterials.0c01761

90. Tian S, Stevens R, McInnes B, Lewinski N. Machine assisted experimentation of extrusion-based bioprinting systems. *Micromachines (Basel)*. 2021;12(7):780.

doi: 10.3390/mi12070780

91. Kelly D, Sergis V, Ventura i Blanco L, Mason K, Daly AC. Autonomous control of extrusion bioprinting using convolutional neural networks. *Adv Funct Mater*. 2025;35(30):2424553.

doi: 10.1002/adfm.202424553

92. Usseglio N, González Santos A, Fernández Ferrer A, Flores J, Nieto D. High-fidelity "top-down" DLP bioprinting of multi-material soft tissue constructs enabled by computer vision-based layer control. *Biofabrication*. 2026;18(2):025013.

doi: 10.1088/1758-5090/ae55cc

93. Arduengo J, Hascoët N, Chinesta F, Hascoet J. Closed-loop control of extrusion-based bioprinting through real-time computer vision. *J Mach Eng*. 2025;25(2):28-42.

doi: 10.36897/jme/205422

94. Brion DAJ, Pattinson SW. Generalisable 3D printing error detection and correction via multi-head neural networks. *Nat Commun*. 2022;13:4654.

doi: 10.1038/s41467-022-31985-y

95. Zhang C, Elvitigala KCML, Mubarok W, Okano Y, Sakai S. Machine learning-based prediction and optimisation framework for as-extruded cell viability in extrusion-based 3D bioprinting. *Virtual Phys Prototyp*. 2024;19(1):e2400330.

doi: 10.1080/17452759.2024.2400330

96. Mohammadrezaei D, Podina L, De Silva J, Kohandel M. Cell viability prediction and optimization in extrusion-based bioprinting via neural network-based Bayesian optimization models. *Biofabrication*. 2024;16(2):025016.

doi: 10.1088/1758-5090/ad17cf

97. Xu H, Liu Q, Casillas J, *et al*. Prediction of cell viability in dynamic optical projection stereolithography-based bioprinting using machine learning. *J Intell Manuf*. 2022;33(4):995-1005.

doi: 10.1007/s10845-020-01708-5

98. Guan J, Sun Y, Yao E, *et al*. Machine learning-assisted stiffness prediction in high-cell-density bioprinting. *Bio-Des Manuf*. 2025;8(4):543-557.

doi: 10.1631/bdm.2400454

99. Kiratitanaporn W, Guan J, Berry D, Lao A, Chen S. Multimodal three-dimensional printing for micro-modulation of scaffold stiffness through machine learning. *Tissue Eng Part A*. 2024;30(11-12):280-292.

doi: 10.1089/ten.tea.2023.0193

100. Kiratitanaporn W, Guan J, Tang M. 3D printing of a biomimetic myotendinous junction assisted by artificial intelligence. *Biomater Sci*. 2024;12(23):6047-6062.

doi: 10.1039/d4bm00892h

101. Guan J, You S, Xiang Y, *et al*. Compensating the cell-induced light scattering effect in light-based bioprinting using deep learning. *Biofabrication*. 2022;14(1):015011.

doi: 10.1088/1758-5090/ac3b92

102. Tang M, Jiang S, Huang X, *et al*. Integration of 3D bioprinting and multi-algorithm machine learning identified glioma susceptibilities and microenvironment characteristics. *Cell Discov*. 2024;10:39.

doi: 10.1038/s41421-024-00650-7

103. Bracco F, Zanderigo G, Paynabar K, Colosimo B. Leveraging transfer learning for efficient bioprinting. *Biofabrication*. 2025;17(3):035022.

doi: 10.1088/1758-5090/ade62f

104. Shin J, Kang R, Hyun K, *et al*. Machine learning-enhanced optimization for high-throughput precision in cellular droplet bioprinting. *Adv Sci (Weinh)*. 2025;12(20):e2412831.

doi: 10.1002/advs.202412831

105. Tröndle K, Miotto G, Rizzo L, *et al*. Deep learning-assisted nephrotoxicity testing with bioprinted renal spheroids. *Int J Bioprint*. 2022;8(2):528.

doi: 10.18063/ijb.v8i2.528

106. Madika B, Saha A, Kang C, *et al*. Artificial intelligence for materials discovery, development, and optimization. *ACS Nano*. 2025;19(30):27116-27158.

doi: 10.1021/acsnano.5c04200

107. Liu W, Zhang Y, Lyu Y, Bosiakov S, Liu Y. Inverse design of anisotropic bone scaffold based on machine learning and regenerative genetic algorithm. *Front Bioeng Biotechnol*. 2023;11:1241151.

doi: 10.3389/fbioe.2023.1241151

108. Peng B, Wei Y, Qin Y, *et al*. Machine learning-enabled constrained multi-objective design of architected materials. *Nat Commun*. 2023;14:6630.

doi: 10.1038/s41467-023-42415-y

109. Verheyen C, Uzel S, Kurum A, Roche E, Lewis J. Integrated data-driven modeling and experimental optimization of granular hydrogel matrices. *Matter*. 2023;6(3):1015-1036.

doi: 10.1016/j.matt.2023.01.011

110. Xu Y, Sarah R, Habib A, Liu Y, Khoda B. Constraint based Bayesian optimization of bioink precursor: a machine learning framework. *Biofabrication*. 2024;16(4):045031.

doi: 10.1088/1758-5090/ad716e

111. Breiman L. Random forests. *Mach Learn*. 2001;45:5-32.

doi: 10.1023/A:1010933404324

112. Cortes C, Vapnik V. Support-vector networks. *Mach Learn*. 1995;20(3):273-297.

doi: 10.1023/A:1022627411411

113. Snoek J, Larochelle H, Adams R. Practical Bayesian optimization of machine learning algorithms. In: Pereira F, Burgers CJ, Bottou L, Weinberger K, eds. *Advances in Neural Information Processing Systems 25 (NIPS 2012)*. Red Hook, NY: Neural Information Processing Systems Foundation, Inc.; 2012.

114. Lookman T, Balachandran P, Xue D, Yuan R. Active learning in materials science with emphasis on adaptive sampling using uncertainties for targeted design. *NPJ Comput Mater*. 2019;5:21.

doi: 10.1038/s41524-019-0153-8

115. Karniadakis G, Kevrekidis I, Lu L, Perdikaris P, Wang S, Yang L. Physics-informed machine learning. *Nat Rev Phys*. 2021;3(6):422-440.

doi: 10.1038/s42254-021-00314-5

116. Shi J, Song J, Song B, Lu WF. Multi-objective optimization design through machine learning for drop-on-demand bioprinting. *Engineering*. 2019;5(3):586-593.

doi: 10.1016/j.eng.2018.12.009

117. Shi J, Wu B, Song J, Li S, Trau D, Lu W. Learning-based cell injection control for precise drop-on-demand cell printing. *Ann Biomed Eng*. 2018;46(9):1267-1279.

doi: 10.1007/s10439-018-2054-2

118. Piotrowska U, Tsoi J, Singh P, Banerjee A, Sobczak M. 3D bioprinting and artificial intelligence for tumor microenvironment modeling: a scoping review of models, methods, and integration pathways. *Mol Pharm*. 2025;22(10):5801-5823.

doi: 10.1021/acs.molpharmaceut.5c01062

119. Babaei M, Shamouil A, Wang J, *et al*. Automated cell properties toolbox from 3D bioprinted hydrogel scaffolds via deep learning and optical coherence tomography. *Biomed Opt Express*. 2025;16(5):2061-2076.

doi: 10.1364/BOE.550401

120. Kassis T, Hernandez-Gordillo V, Langer R, Griffith L. OrgaQuant: human intestinal organoid localization and quantification using deep convolutional neural networks. *Sci Rep*. 2019;9:12479.

doi: 10.1038/s41598-019-48874-y

121. Bian X, Li G, Wang C. A deep learning model for detection and tracking in high-throughput images of organoid. *Comput Biol Med*. 2021;134:104490.

doi: 10.1016/j.compbiomed.2021.104490

122. Beghin A, Grenci G, Sahni G. Automated high-speed 3D imaging of organoid cultures with multi-scale phenotypic quantification. *Nat Methods*. 2022;19(7):881-892.

doi: 10.1038/s41592-022-01508-0

123. Matthews J, Schuster B, Kashaf S. OrganoID: a versatile deep learning platform for tracking and analysis of single-organoid dynamics. *PLoS Comput Biol*. 2022;18(11):e1010584.

doi: 10.1371/journal.pcbi.1010584

124. Branco F, Cunha J, Mendes M, Sousa J, Vitorino C. 3D bioprinting models for glioblastoma: from scaffold design to therapeutic application. *Adv Mater*. 2025;37(18):e2501994.

doi: 10.1002/adma.202501994

125. Tang M, Xie Q, Gimple RC, *et al*. Three-dimensional bioprinted glioblastoma microenvironments model cellular dependencies and immune interactions. *Cell Res*. 2020;30(10):833-853.

doi: 10.1038/s41422-020-0338-1

126. Tan S, Ding Y, Wang W. Development of an AI model for DILI-level prediction using liver organoid brightfield images. *Commun Biol*. 2025;8:886.

doi: 10.1038/s42003-025-08205-6

127. Zhang C, Meyer S, O'Meara M. A human liver organoid screening platform for DILI risk prediction. *J Hepatol*. 2023;78(5):998-1006.

doi: 10.1016/j.jhep.2023.01.019

128. Li Z, Li K, Zhang C. Bioprinted organoids: an innovative engine in biomedicine. *Adv Sci (Weinh)*. 2025;12(33):e07317.

doi: 10.1002/advs.202507317

129. Tobias A, Wahab A. Autonomous "self-driving" laboratories: a review of technology and policy implications. *R Soc Open Sci*. 2025;12(7):250646.

doi: 10.1098/rsos.250646

130. Tom G, Schmid SP, Baird SG, *et al*. Self-driving laboratories for chemistry and materials science. *Chem Rev*. 2024;124(16):9633-9732.

doi: 10.1021/acs.chemrev.4c00055

131. Coley C, Eyke N, Jensen K. Autonomous discovery in the chemical sciences part I: progress. *Angew Chem Int Ed Engl*. 2020;59(51):22858-22893.

doi: 10.1002/anie.201909987

132. Abolhasani M, Kumacheva E. The rise of self-driving labs in chemical and materials sciences. *Nat Synth*. 2023;2(6):483-492.

doi: 10.1038/s44160-022-00231-0

133. An J, Chua C, Mironov V. Application of machine learning in 3D bioprinting: focus on development of big data and digital twin. *Int J Bioprint*. 2021;7(1):342.

doi: 10.18063/ijb.v7i1.342

134. Yu S, Luo Y, Chen S, Fan J, Zhang H. Quantitative assessment of hydrogel printability in extrusion bioprinting. *Gels*. 2026;12(3):189.

doi: 10.3390/gels12030189

135. Lookman T, Liu Y, Gao Z. Materials informatics: emergence to autonomous discovery in the age of AI. *Adv Mater*. 2026;38(29):e15941.

doi: 10.1002/adma.202515941

136. Formica FA, Wu E, Brey L, *et al*. Bridging innovation and efficiency: the promises and challenges of self-driving labs as sustainable drivers for chemistry. *Chimia (Aarau)*. 2025;79(9):600-605.

doi: 10.2533/chimia.2025.600

137. Lee H, Yoo HJ, Jang HS, Park B, Park YJ, Han SS. Toward self-driving laboratory 2.0 for chemistry and materials discovery. *Mater Horiz*. 2026;13:4712-4739.

doi: 10.1039/d5mh01984b

138. Szymanski NJ, Zeng Y, Huo H, Bartel CJ, Kim H, Ceder G. Toward autonomous design and synthesis of novel inorganic materials. *Mater Horiz*. 2021;8(8):2169-2198.

doi: 10.1039/d1mh00495f